

Chemistry of C-Trimethylsilyl-Substituted Heterocarboranes. 19. Synthetic and Structural Studies on Trinuclear Ln(III) Carborane Clusters [Ln(III) = Sm, Gd, Tb, Dy, Ho]. I. Conversion to Sandwiched Manganese(II) and Cobalt(III) Carborane Complexes

Narayan S. Hosmane,^{*,†} Ying Wang, Aderemi R. Oki, Hongming Zhang, and John A. Maguire

Department of Chemistry, Southern Methodist University, Dallas, Texas 75275

Received September 1, 1995[Ⓢ]

The reaction of *closo-exo*-4,5-Li(THF)₂-1-Li(THF)₂-2,3-(SiMe₃)₂-C₂B₄H₄ with anhydrous LnCl₃ (Ln = Sm, Gd, Tb, Dy, Ho), in a molar ratio of 2:1 in dry benzene (C₆H₆), produced the sandwiched paramagnetic species { $[\eta^5\text{-1-Ln-2,3-(SiMe}_3\text{)}_2\text{-2,3-C}_2\text{B}_4\text{H}_4\text{]}_3\{[\mu_2\text{-1-Li-2,3-(SiMe}_3\text{)}_2\text{-2,3-C}_2\text{B}_4\text{H}_4\text{]}_3(\mu_3\text{-OME})\}[\mu_2\text{-Li(C}_4\text{H}_8\text{O)}\text{]}_3(\mu_3\text{-O})\}$ (Ln = Sm (**1**), Gd (**2**), Tb (**3**), Dy (**4**), Ho (**5**)) in 59%, 58%, 49%, 52%, and 59% yields, respectively. All compounds were characterized by IR spectroscopy and by single-crystal X-ray diffraction studies; compound **1** was also characterized by ¹H, ¹¹B, and ¹³C NMR spectroscopy. Compounds **1**–**5** are isostructural clusters consisting of three half-sandwich lanthanacarboranes, three lithiacarboranes, three bridging lithium atoms, and three THF molecules of solvation. Their structures are such that the nine metal atoms form a tricapped trigonal prism with the lanthanide metals at the capping positions. The reaction of **2** with MnCl₂ in benzene, followed by the addition of TMEDA, gave a dinuclear manganacarborane sandwich complex, 4,4',5,5'-Mn(TMEDA)-1,1'-*commo*-Mn[2,3-(SiMe₃)₂-2,3-C₂B₄H₄]₂ (**6**). Compound **6** was characterized on the basis of its elemental analysis and IR spectrum and also by X-ray diffraction. The reaction of **1** with CoCl₂ in dry benzene, followed by the addition of TMEDA, gave the cobalt(III) sandwich complex, Li(TMEDA)₂{1,1'-*commo*-Co[2,3-(SiMe₃)₂-2,3-C₂B₄H₄]₂} (**7**). Complex **7** was characterized on the basis of ¹H, ⁷Li, ¹¹B, and ¹³C NMR spectra and IR spectra and also by X-ray diffraction.

Introduction

The metallacarboranes are a class of organometallic compounds in which metal moieties are incorporated into the polyhedral structures of carborane cages. Much of the early, and present, interest in such compounds was derived from the recognition by Hawthorne that the frontier orbitals of the *nido*-carborane dianion, [C₂R₂B₉H₉]²⁻ (R = H or a cage carbon substituent), should be similar to those of the cyclopentadienide ion, [C₅R₅]⁻.¹ The parallel between the metallocenes and the metallacarboranes has been demonstrated through numerous reports of the results of synthetic and structural studies involving primarily the icosahedral, MC₂B₉, or the pentagonal bipyramidal, MC₂B₄, cage compounds.^{2,3} The majority of these investigations have been on the p-block or d-block metal sandwich or half-sandwich metallacarboranes, with the f-block metal complexes receiving much less attention. The first

reported lanthanacarborane was the uranacarborane dianion, [U(C₂B₉H₁₁)₂Cl₂]²⁻, described in 1977 by Raymond and co-workers.⁴ The structure was very similar to that of the Cp₂MCl₂ metallocenes, in that it showed a bent-sandwich structure in which two [C₂B₉H₁₁]²⁻ ligands were η⁵-bonded to U(IV), which was also coordinated by two Cl⁻ ligands. In a series of recent papers, Hawthorne *et al.* reported the syntheses and structures of the sandwich and half-sandwich complexes of several divalent and trivalent lanthanide metals with the [C₂B₉H₁₁]²⁻ and [C₂B₁₀H₁₂]²⁻ ligands.^{5–8} In the [C₂B₉H₁₁]²⁻ ligand system, half-sandwich compounds of the type Ln(C₂B₉H₁₁)(THF)₄ were obtained with the divalent lanthanides, while the trivalent metals gave bent sandwich anionic complexes, similar in structure to the uranacarborane.^{5,6} However, the results for the larger [C₂B₁₀H₁₂]²⁻ ligand were more complex, with the products depending on both the nature of the lanthanide and the metal-to-carborane molar ratios used in the reactions.^{7,8} In general, polymeric structures were obtained from 1:1 molar reaction stoichiometries,

[†] Camille and Henry Dreyfus Scholar awardee.

[Ⓢ] Abstract published in *Advance ACS Abstracts*, December 15, 1995.

(1) Hawthorne, M. F.; Young, D. C.; Andrews, T. D.; Howe, D. V.; Pilling, R. L.; Pitts, A. D.; Reintjes, M.; Warren, L. F., Jr.; Wegner, P. A. *J. Am. Chem. Soc.* **1968**, *90*, 879 and references therein.

(2) For summaries see: (a) Hawthorne, M. F. In *Advances in Boron and the Boranes [Mol. Struct. Energ., Vol. 5]*; Liebman, J. F.; Greenberg, A.; Williams, R. E., Eds.; VCH Publishers, Inc.: New York, 1988; Chapter 11, pp 225–233. (b) Grimes, R. N. In *Comprehensive Organometallic Chemistry*; Wilkinson, G.; Stone, F. G. A., Abel, E. W., Eds.; Pergamon: Oxford, 1982; Chapter 5.5. (c) Grimes, R. N. *Chem. Rev.* **1992**, *92*, 251.

(3) Hosmane, N. S.; Maguire, J. A. *J. Cluster Sci.* **1993**, *4*, 297 and references therein.

(4) Fronczek, F. R.; Halstead, G. W.; Raymond, K. N. *J. Am. Chem. Soc.* **1977**, *99*, 1769.

(5) Manning, M. J.; Knobler, C. B.; Hawthorne, M. F. *J. Am. Chem. Soc.* **1988**, *110*, 4458.

(6) Manning, M. J.; Knobler, C. B.; Khattar, R.; Hawthorne, M. F. *Inorg. Chem.* **1991**, *30*, 2009.

(7) Khattar, R.; Knobler, C. B.; Johnson, S. E.; Hawthorne, M. F. *Inorg. Chem.* **1991**, *30*, 1970.

(8) Khattar, R.; Manning, M. J.; Knobler, C. B.; Johnson, S. E.; Hawthorne, M. F. *Inorg. Chem.* **1992**, *31*, 268.

Table 1. Preparation of
 $\{[\eta^5\text{-1-Ln-2,3-(SiMe}_3)_2\text{-2,3-C}_2\text{B}_4\text{H}_4]_3[(\mu_2\text{-1-Li-2,3-(SiMe}_3)_2\text{-2,3-C}_2\text{B}_4\text{H}_4)_3(\mu_3\text{-OMe})][\mu_2\text{-Li(C}_4\text{H}_8\text{O})]_3(\mu_3\text{-O})\}$

compd	LnCl ₃ (g, mmol)	dilithiacarborane: ^a g, mmol	color	mp (°C)	yield: ^b g, mmol, (%)
1	SmCl ₃ (0.7, 2.73)	2.86, 5.5	yellow	171–173	1.17, 0.54, 59
2	GdCl ₃ (0.84, 3.18)	3.33, 6.4	colorless	100–103	1.35, 0.61, 58
3	TbCl ₃ (0.66, 2.5)	2.6, 5.0	yellow	150	0.9, 0.41, 49
4	DyCl ₃ (0.81, 3.01)	3.12, 6.0	pale yellow	>250	1.16, 0.52, 52
5	HoCl ₃ (0.68, 2.5)	2.6, 5.0	white	>240	1.10, 0.49, 59

^a *closo-exo-4,5-Li(THF)₂-1-Li(THF)₂-2,3-(SiMe₃)₂-2,3-C₂B₄H₄*. ^b Based on LnCl₃ as the limiting reagent and $\{[\eta^5\text{-1-Ln-2,3-(SiMe}_3)_2\text{-2,3-C}_2\text{B}_4\text{H}_4]_3[(\mu_2\text{-1-Li-2,3-(SiMe}_3)_2\text{-2,3-C}_2\text{B}_4\text{H}_4)_3(\mu_3\text{-OMe})][\mu_2\text{-Li(C}_4\text{H}_8\text{O})]_3(\mu_3\text{-O})\} \cdot 1.5\text{C}_6\text{H}_6$ as the product.

while, at least in the case of europium, excess carborane resulted in a bent sandwich Eu(II) complex, similar in structure to those obtained in the C₂B₉ system.^{7,8} It is of interest to note that no direct reactions between either carborane ligand and a Ln(III) salt have been described.

There is even less information available on the lanthanacarboranes of the smaller C₂B₄-cage system. The reaction of the TMEDA-solvated dilithium compound of the [2,3-(SiMe₃)₂-2,3-C₂B₄H₄]²⁻ anion with anhydrous ErCl₃, in a 2:1 molar ratio, produced a bent-sandwich complex, [Li(TMEDA)₂][1-Cl-1-(μ-Cl)-2,2',3,3'-(SiMe₃)₄-5,6-[(μ-H)₂Li(TMEDA)]-4,4',5'-[(μ-H₃)Li(TMEDA)]-*commo*-Er(2,3-C₂B₄H₄)₂], which underwent a ligand exchange with the "carbons apart" carborane anion, [2,4-(SiMe₃)₂-2,4-C₂B₄H₄]²⁻, to give a dimeric, mixed-ligand bent-sandwich complex.⁹ On the other hand, the results were quite different when the THF-solvated dilithiacarboranes were involved. In our preliminary reports it was shown that the reaction of the THF-solvated dilithium compound of the [2,3-(SiMe₃)₂-2,3-C₂B₄H₄]²⁻ anion with either anhydrous GdCl₃ or TbCl₃ produced a trinuclear lanthanacarborane cluster.^{10,11} In order to establish the extent of this reactivity pattern, we have carried out reactions of the THF-solvated dilithium compound of the SiMe₃-substituted C₂B₄-carborane ligand with a number of LnCl₃ salts. Here we report, in detail, the preparation, characterization, and molecular structures of the products when Ln = Sm, Gd, Tb, Dy, and Ho. The reactivities of these lanthanacarboranes have been investigated by studying the reaction of the gadolinacarborane with MnCl₂ and samaracarborane with CoCl₂, and the results are reported herein.

Experimental Section

Materials. The preparation of 2,3-bis(trimethylsilyl)-2,3-dicarba-*nido*-hexaborane(8) followed literature methods.¹² Prior to use, SmCl₃, GdCl₃, TbCl₃, DyCl₃, and HoCl₃ (Strem) and MnCl₂ and CoCl₂ (Aldrich) were heated to 130 °C under vacuum for 24 h. Benzene, tetrahydrofuran (THF), and *n*-hexane were dried over LiAlH₄ and doubly distilled before use. All other solvents were dried over 4–8 mesh molecular sieves (Aldrich) and either saturated with dry argon or degassed before use; *t*-butyllithium, *t*-BuLi (1.7 M solution in pentane obtained from Aldrich), was used as received.

Spectroscopic Procedure. Proton, lithium-7, boron-11, and carbon-13 pulse Fourier transform NMR spectra, at 200,

77.7, 64.2, and 50.3 MHz, respectively, were recorded on an IBM-200 SY multinuclear NMR spectrometer. Infrared spectra were recorded on a Perkin-Elmer Model 283 infrared spectrometer, a Perkin-Elmer Model 1600 FT-IR spectrophotometer, or a Nicolet Magna 550 FT-IR spectrophotometer. Elemental analyses were obtained from E+R Microanalytical Laboratory, Inc., Corona, NY.

Synthetic Procedures. All experiments were carried out in Pyrex glass round-bottom flasks of 250- or 100-mL capacity, containing magnetic stirring bars and fitted with high-vacuum Teflon valves. Nonvolatile substances were manipulated in either a drybox or evacuable glovebags under an atmosphere of dry nitrogen. All known compounds among the products were identified by comparing their IR and ¹H NMR spectra with those of authentic samples.

Synthesis of $\{[\eta^5\text{-1-Ln-2,3-(SiMe}_3)_2\text{-2,3-C}_2\text{B}_4\text{H}_4]_3[(\mu_2\text{-1-Li-2,3-(SiMe}_3)_2\text{-2,3-C}_2\text{B}_4\text{H}_4)_3(\mu_3\text{-OMe})][\mu_2\text{-Li(C}_4\text{H}_8\text{O})]_3(\mu_3\text{-O})\}$ [Ln = Sm (1), Gd (2), Tb (3), Dy (4) and Ho (5)]. The methods, solvents, and reaction times for the preparation of **1–5** were all the same, so only a typical synthesis of $\{[\eta^5\text{-1-Ln-2,3-(SiMe}_3)_2\text{-2,3-C}_2\text{B}_4\text{H}_4]_3[(\mu_2\text{-1-Li-2,3-(SiMe}_3)_2\text{-2,3-C}_2\text{B}_4\text{H}_4)_3(\mu_3\text{-OMe})][\mu_2\text{-Li(C}_4\text{H}_8\text{O})]_3(\mu_3\text{-O})\}$ will be described. Details of quantities used and product yields are given in Table 1. The dilithiacarborane *closo-exo-4,5-Li(THF)₂-1-Li(THF)₂-2,3-(SiMe₃)₂-2,3-C₂B₄H₄* was prepared by the reaction of a measured quantity of *nido-2,3-(SiMe₃)₂-2,3-C₂B₄H₆* with *t*-BuLi in a THF solution, as described elsewhere.¹³ The THF solvent was removed, *in vacuo*, the resulting solid product was redissolved in dry benzene (30 mL), and the solution was reacted with anhydrous LnCl₃, in a molar ratio of 2:1, for 5 h at 0 °C and then at room temperature for a further period of 24 h, with constant stirring. During this time the solution became turbid and turned light yellow in color. The heterogeneous reaction mixture was filtered through a frit. The dark residue remaining on the frit after repeated washing with anhydrous benzene was discarded. Removal of the solvent, *in vacuo*, from the filtrate and the combined washings yielded an air-sensitive solid product, which was recrystallized from benzene solution and was identified as the trinuclear lanthanacarborane cluster $\{[\eta^5\text{-1-Ln-2,3-(SiMe}_3)_2\text{-2,3-C}_2\text{B}_4\text{H}_4]_3[(\mu_2\text{-1-Li-2,3-(SiMe}_3)_2\text{-2,3-C}_2\text{B}_4\text{H}_4)_3(\mu_3\text{-OMe})][\mu_2\text{-Li(C}_4\text{H}_8\text{O})]_3(\mu_3\text{-O})\}$.

Spectroscopic data for complex **1**: ¹H NMR (C₄D₈O, external Me₄Si) δ 3.58 [s, 12H, THF], 1.73 [s, 12H, THF], 1.23 [s, 3H, OMe], 0.31 [s, 54H, SiMe₃], 0.05 [s, 18H, SiMe₃], -0.011 [s, 18H, SiMe₃], -0.29 [s, 18H, SiMe₃]; ¹¹B NMR (C₄D₈O, external BF₃·OEt₂) δ 20.25 [br, ill-defined peak, 1B, basal BH, ¹J(¹¹B–¹H) = unresolved], 7.47 [br, ill-defined peak, 1B, basal BH, ¹J(¹¹B–¹H) = unresolved], 0.76 [br, ill-defined peak, 1B, basal BH, ¹J(¹¹B–¹H) = unresolved], -17.58 [br, ill-defined peak, 1B, apical BH, ¹J(¹¹B–¹H) = unresolved]; ¹³C NMR (C₄D₈O, external Me₄Si) δ ~100–110 [s (v br), cage carbons (SiCB)], 68.80 [t, THF, ¹J(¹³C–¹H) = 147.5 Hz], 25.25 [t, THF, ¹J(¹³C–¹H) = 133.6 Hz], 3.97 [q, SiMe₃, ¹J(¹³C–¹H) = ~119–120 Hz], 3.40 [q, SiMe₃, ¹J(¹³C–¹H) = ~119–120 Hz], 2.84 [q, SiMe₃, ¹J(¹³C–¹H) = ~119–120 Hz], 2.03 [q, SiMe₃, ¹J(¹³C–¹H) = ~119–120 Hz]. The paramagnetism of **2–5** precluded obtain-

(9) Hosmane, N. S.; Wang, Y.; Zhang, H.; Oki, A. R.; Maguire, J. A.; Waldhör, E.; Kaim, W.; Binder, H.; Kremer, R. K. *Organometallics* **1995**, *14*, 1101.

(10) Oki, A. R.; Zhang, H.; Hosmane, N. S. *Angew. Chem., Int. Ed. Engl.* **1992**, *31*, 432.

(11) Zhang, H.; Oki, A. R.; Wang, Y.; Maguire, J. A.; Hosmane, N. S. *Acta Crystallogr., Cryst. Struct. Commun.* **1995**, *C51*, 635.

(12) (a) Hosmane, N. S.; Sirmokadam, N. N.; Mollenhauer, M. N. *J. Organomet. Chem.* **1985**, *279*, 359. (b) Hosmane, N. S.; Mollenhauer, M. N.; Cowley, A. H.; Norman, N. C. *Organometallics* **1985**, *4*, 1194.

(13) (a) Barreto, R. D.; Hosmane, N. S. *Inorg. Synth.* **1992**, *29*, 89. (b) Hosmane, N. S.; Sexena, A. K.; Barreto, R. D.; Maguire, J. A.; Jia, L.; Wang, Y.; Oki, A. R.; Grover, K. V.; Whitten, S. J.; Dawson, K.; Tolle, M. A.; Siriwardane, U.; Demissie, T.; Fagner, J. S. *Organometallics* **1993**, *12*, 3001.

Table 2. Infrared Absorptions (cm⁻¹; C₆D₆ vs C₆D₆)^a

compd	absorption
1	2945 (vs), 2880 (vs), [ν(C-H)], 2515 (vs, s), 2450 (vs, br), 2260 (vs, s) [ν(BH)], 1600 (w, br), 1480 (ms) [δ(CH) _{asym}], 1385 (ms), 1325 (s), 1245 (vs) [δ(CH) _{sym}], 1160 (s, br), 1080 (s), 845 (vvs,br) [ρ(CH)], 750 (s), 670 (s), 620 (s), 480 (vs, br), 420 (w, br)
2	2944 (vs), 2875 (vs) [ν(C-H)], 2350 (s, br), 2330 (s), 2280 (s, br) [ν(B-H)], 1230 (s), 1170 (s), 1020 (s), 845 (vs, br), 748 (s), 660 (s), 620 (w), 420 (w)
3	2959 (vs), 2950 (vs), 2899 (vs) [ν(C-H)], 2600 (w), 2450 (w br) [ν(B-H)], 1700 (sh), 1455 (s), 1449 (s), 1327 (s), 1249 (s), 1200 (s), 1161 (w), 856 (ms), 810 (ms), 804 (m)
4	2959.8 (s), 2858 (vs), 2817 (ms) [ν(C-H)], 2522 (br, s), 2388 (ms), 2279 (vs, s) [ν(BH)], 1618 (s), 1455 (ms) [δ(CH) _{asym}], 1330 (ms), 1287 (w), 1261 (s) [δ(CH) _{sym}], 1097 (s, br), 1020 (s), 813 (vvs, br) [ρ(CH)], 757 (w), 687 (w), 625 (w), 586 (w)
5	3088 (vs), 3070 (vs), 3038 (s), 3025 (vs), 2987 (vs), 2947 (s), 2930 (s), 2888 (vs), 2858(s) [ν(C-H)], 2528 (vs, s), 2486 (vs, br), 2466 (vs, s) [ν(BH)], 1810 (ms), 1616 (ms, br), 1474 (ms) [δ(CH) _{asym}], 1399 (ms), 1362 (s), 1318 (vs) [δ(CH) _{sym}], 1200 (s, br), 845 (vvs, br) [ρ(CH)], 750 (s), 670 (s)
6	2966 (ms), 2900 (w), 2845 (w) [ν(C-H)], 2528 (s), 2460 (s), 2260 (s) [ν(B-H)], 1458 (s) [δ(CH) _{asym}], 1333 (s), 1250 (vs) [δ(CH) _{sym}], 1181 (s), 1158 (s), 840 (vvs, br) [ρ(CH)], 750 (mw), 623 (w)
7	2950 (s), 2924 (s), 2898 (m), 2859 (m), 2800 (m) [ν(C-H)], 2532 (m) [ν(BH)], 1611 (w, s), 1515 (m, s), 1470 (ms, br), 1405 (s, s), [δ(CH) _{asym}], 1386 (m, s), 1360 (m, s), 1251 (vs) [δ(CH) _{sym}], 1186 (m, br), 1058 (s, br), 1019 (br), 839 (vs, br) [ρ(CH)], 800 (m, s), 632(m, s), 485 (s)

^a Legend: v = very, s = strong or sharp, m = medium, w = weak, sh = shoulder, and br = broad.

ing their useful NMR spectra. The infrared spectral data with selected assignments for **1–5** are presented in Table 2. Anal. Calcd for [C₆₁H₁₅₉B₂₄O₅Si₁₂Li₆Sm₃]·1.5[C₆H₆] (**1**): C, 38.58; H, 7.77. Found: C, 38.73; H, 7.71. Calcd for [C₆₁H₁₅₉B₂₄O₅Si₁₂Li₆Gd₃]·1.5[C₆H₆] (**2**): C, 38.22; H, 7.70. Found: C, 38.40; H, 7.89. Calcd for [C₆₁H₁₅₉B₂₄O₅Si₁₂Li₆Tb₃]·1.5[C₆H₆] (**3**): C, 38.13; H, 7.68. Found: C, 38.49; H, 7.80. Calcd for [C₆₁H₁₅₉B₂₄O₅Si₁₂Li₆Dy₃]·1.5[C₆H₆] (**4**): C, 37.95; H, 7.64. Found: C, 37.85; H, 7.62. Calcd for [C₆₁H₁₅₉B₂₄O₅Si₁₂Li₆Ho₃]·1.5[C₆H₆] (**5**): C, 37.82; H, 7.62. Found: C, 38.13; H, 7.80.

Synthesis of 4,4',5,5'-Mn(TMEDA)-1,1'-commo-Mn[2,3-(SiMe₃)₂-2,3-C₂B₄H₄]₂ (6**).** When **2** (0.425 g, 0.19 mmol) was reacted with anhydrous MnCl₂ (0.038 g, 0.3 mmol) in a dry benzene solution (20 mL) at room temperature for 24 h, the solution became turbid and turned dark-brown in color. The solution was filtered through a frit in *vacuo*, and about 1.5 mL of dry TMEDA was added to the filtrate which caused the immediate precipitation of a dark red crystalline solid, identified as 4,4',5,5'-Mn(TMEDA)-1,1'-commo-Mn[2,3-(SiMe₃)₂-2,3-C₂B₄H₄]₂ (**6**) (0.07 g, 0.106 mmol; 70% yield; mp > 240 °C; soluble in both polar and nonpolar organic solvents). The mother liquor contained unreacted **2** (0.3 g, 0.14 mmol), which was isolated by concentrating the mother liquor and by subsequent crystallization. The paramagnetism of the compound prevented the collection of reliable NMR data; the IR spectral data are given in Table 2. Anal. Calcd for C₂₂H₅₂N₂B₈Si₄Mn₂: C, 40.44; H, 8.02; N, 4.29. Found: C, 40.29; H, 8.16; N, 4.21.

Synthesis of Li(THF)₄{1,1'-commo-Co[2,3-(SiMe₃)₂-2,3-C₂B₄H₄]₂} (7a**).** When **1** (1.5 g, 0.69 mmol) was reacted with anhydrous CoCl₂ (0.22 g, 1.05 mmol) in a dry benzene solution (20 mL) at room temperature for 24 h, the solution became turbid and turned reddish brown in color. The solution was filtered through a frit, and the solvent was removed from the filtrate, in *vacuo*. The reddish brown residue was redissolved in a mixture of 5% THF and 95% hexane, slow evaporation of which yielded a red crystalline solid, identified as Li(THF)₄{1,1'-commo-Co[2,3-(SiMe₃)₂-2,3-C₂B₄H₄]₂} (**7a**) (0.47 g, 0.6 mmol; 57%, mp 120 °C dec; soluble in both polar and nonpolar organic solvents). The mother liquor also contained unreacted **1** (0.73 g, 0.33 mmol), which was isolated by slow crystallization.

Spectroscopic data for **7a**: ¹H NMR (C₆D₆, relative to external Me₄Si) δ 3.52 [s, 16H, THF], 1.42 [s, 16H, THF], 0.55 [s, 36H, SiMe₃]; ¹¹B NMR (C₆D₆, external BF₃·OEt₂) δ 8.54 [br, ill-defined peak, 1B, basal BH, ¹J(¹¹B-¹H) = unresolved], 0.09 [br, ill-defined peak, 2B, basal BH, ¹J(¹¹B-¹H) = unresolved], -8.90 [br, ill-defined peak, 1B, basal BH, ¹J(¹¹B-¹H) = unresolved], ¹³C NMR (CDCl₃, relative to external Me₄Si) δ 89.8 [s (br), 4C, cage carbons (SiCB)], 68.91 [t, 8 C, THF, ¹J(¹³C-¹H) = 148.0 Hz], 25.42 [t, 8 C, THF, ¹J(¹³C-¹H) = 125.0 Hz], 2.45 [q, 6 C, SiMe₃, ¹J(¹³C-¹H) = 119.3 Hz], 1.37 [q, 6

C, SiMe₃, ¹J(¹³C-¹H) = 119.3 Hz]. Anal. Calcd for C₃₂H₆₈O₄B₈Si₄CoLi: C, 49.18; H, 8.77. Found: C, 49.32; H, 8.03.

Compound **7a** was transformed into the more readily crystallizable complex, Li(TMEDA)₂{1,1'-commo-Co[2,3-(SiMe₃)₂-2,3-C₂B₄H₄]₂} (**7**) by further reaction with TMEDA.

Spectroscopic data for **7**: ¹H NMR (C₆D₆, relative to external Me₄Si) δ 2.0 [s, 8H, TMEDA (CH₂)], 1.88 [s, 24H, TMEDA (CH₃)], 0.58 [s, 36H, SiMe₃]; ¹¹B NMR (C₆D₆, external BF₃·OEt₂) δ 8.26 [br, ill-defined peak, 1B, basal BH, ¹J(¹¹B-¹H) = unresolved], 1.19 [br, ill-defined peak, 2B, basal BH, ¹J(¹¹B-¹H) = unresolved], -8.80 [br, ill-defined peak, 1B, basal BH, ¹J(¹¹B-¹H) = unresolved]; ¹³C NMR (C₆D₆, relative to external Me₄Si) δ 91.0 [s (br), 2 C, cage carbons (SiCB)], 58.1 [t, 2 C, TMEDA, ¹J(¹³C-¹H) = 120.1 Hz], 47.38 [q, 4 C, TMEDA, ¹J(¹³C-¹H) = 120.5 Hz], 4.25 [q, 6C, SiMe₃, ¹J(¹³C-¹H) = 119.4 Hz]; ⁷Li NMR (C₆D₆, relative to external aqueous LiNO₃) δ -1.58 ppm. The IR spectral data are given in Table 2. Anal. Calcd for C₂₈H₆₈N₄B₈Si₄CoLi: C, 46.35; H, 9.44; N, 7.72. Found: C, 46.55; H, 9.78; N, 7.59.

Crystal Structure Analysis of {[η⁵-1-Ln-2,3-(SiMe₃)₂-2,3-C₂B₄H₄]₂[(μ₂-1-Li-2,3-(SiMe₃)₂-2,3-C₂B₄H₄]₂(μ₃-OMe)]-[μ₂-Li(C₄H₈O)]₂(μ₃-O)] [Ln = Sm (1**), Gd (**2**), Tb (**3**), Dy (**4**), Ho (**5**), 4,4',5,5'-Mn(TMEDA)-1,1'-commo-Mn[2,3-(SiMe₃)₂-2,3-C₂B₄H₄]₂ (**6**), and Li(TMEDA)₂{1,1'-commo-Co[2,3-(SiMe₃)₂-2,3-C₂B₄H₄]₂} (**7**).** Pale yellow crystals of the lanthanacarboranes **1–5** and red crystals of **6** and **7** were grown from benzene solutions by slow evaporation. The appropriate crystals were mounted on a Siemens R3m/V diffractometer under a low-temperature nitrogen stream. The pertinent crystallographic data are summarized in Tables 3 and 4. The final unit cell parameters were obtained by least-squares fits of 20–30 accurately centered reflections measured in the 2θ range from 18 to 32°. While compounds **1–5** are isostructural with the *P*₁ space group, **6** crystallized in the monoclinic space group *P*₂/*c*. Although the systematic absences in the diffraction pattern of **7** were consistent with the space groups *P*₄*mc*, *P*₄*2c*, or *P*₄*2*/*mmc*, the subsequent successful refinement of the structure confirmed that *P*₄*2*/*mmc* was the correct space group. Three standard reflections were periodically monitored during the data collection which showed no significant change in intensity. The data were corrected for Lorentz and polarization effects. Semiempirical absorption corrections (based on ψ scans) were applied for each structure; the relevant minimum and maximum transmission factors are listed in Tables 3 and 4. All structures were solved by heavy-atom methods using the SHELXTL-Plus package of programs.¹⁴ The structures **3** and **7** were refined on *F*² for all reflections using

(14) Sheldrick, G. M. *Structure Determination Software programs*; Siemens X-ray Analytical Instruments Corp., Inc.: Madison, WI, 1990.

Table 3. Crystal Data^a for 1–5

	1	2	3	4	5
formula	[C ₆₁ H ₁₅₉ O ₅ B ₂₄ Si ₁₂ -Li ₆ Sm ₃][C ₆ H ₆]	[C ₆₁ H ₁₅₉ O ₅ B ₂₄ Si ₁₂ -Li ₆ Gd ₃][C ₆ H ₆]	[C ₆₁ H ₁₅₉ O ₅ B ₂₄ Si ₁₂ -Li ₆ Tb ₃][C ₆ H ₆]	[C ₆₁ H ₁₅₉ O ₅ B ₂₄ Si ₁₂ -Li ₆ Dy ₃][C ₆ H ₆]	[C ₆₁ H ₁₅₉ O ₅ B ₂₄ Si ₁₂ -Li ₆ Ho ₃][C ₆ H ₆]
fw	2140.2	2160.9	2165.9	2176.7	2183.9
space group	<i>P</i> 1	<i>P</i> 1	<i>P</i> 1	<i>P</i> 1	<i>P</i> 1
<i>a</i> , Å	16.046(7)	16.035(7)	15.976(4)	16.012(5)	16.002(3)
<i>b</i> , Å	16.884(4)	16.883(6)	16.627(4)	16.822(5)	16.823(4)
<i>c</i> , Å	23.905(7)	23.903(9)	23.670(6)	23.779(7)	23.729(6)
α, deg	89.05(2)	89.04(3)	90.08(2)	89.55(2)	89.67(2)
β, deg	88.96(3)	88.87(3)	89.97(2)	89.25(2)	89.26(2)
γ, deg	68.07(3)	67.95(3)	69.16(2)	67.96(2)	68.05(2)
<i>V</i> , Å ³	6006(3)	5996(4)	5876(3)	5936(3)	5924(2)
<i>Z</i>	2	2	2	2	2
<i>D</i> _{calcd} , g cm ⁻³	1.183	1.197	1.224	1.218	1.224
abs coeff, mm ⁻¹	1.603	1.795	1.944	2.026	2.141
cryst dmns, mm	0.35 × 0.20 × 0.10	0.25 × 0.15 × 0.30	0.25 × 0.10 × 0.05	0.20 × 0.30 × 0.05	0.25 × 0.10 × 0.05
scan type	θ/2θ	ω/2θ	θ/2θ	ω/2θ	ω/2θ
scan sp in ω: min, max	6.0, 30.0	5.0, 25.0	6.0, 30.0	6.0, 30.0	10.0, 30.0
2θ range, deg	3.5–38.0	3.5–38.0	3.5–40.0	3.5–40.0	3.5–44.0
<i>T</i> , K	230	230	230	230	230
decay, %	0	0	0	0	0
data collcd	10 154	10 077	11 202	11 273	15 266
obsd reflns, <i>F</i> > 6.0σ(<i>F</i>)	8463	8156	9679	8377	9959
params refined	1012	987	1079	732	987
GOF	2.42	2.43	1.05	3.05	1.57
Δρ(max, min), e/Å ³	1.08, -0.62	1.27, -1.04	1.12, -0.70	2.72, -1.80	1.37, -1.15
<i>R</i> ^b	0.045	0.048	0.029	0.078	0.052
w <i>R</i>	0.069 ^c	0.071 ^c	w <i>R</i> ₂ = 0.074 ^d	0.107 ^c	0.061

^a Graphite monochromatized Mo Kα radiation, λ = 0.710 73 Å. ^b $R = \sum ||F_o| - |F_c|| / \sum |F_o|$, w*R* = $[\sum w(F_o - F_c)^2 / \sum w(F_o)^2]^{1/2}$. ^c $w = 1/[\sigma^2(F_o) + 0.001(F_o)^2]$. ^d $w = 1/[\sigma^2(F_o^2) + (0.0410P)^2 + 14.4051P]$, where $P = (F_o^2 + 2F_c^2)/3$.

Table 4. Crystal Data^a for 6 and 7

	6	7
formula	C ₂₂ H ₆₀ N ₂ B ₈ Si ₄ Mn ₂	[C ₂₈ H ₇₆ N ₄ B ₈ Si ₂ -LiCo][C ₆ H ₆]
fw	661.4	811.7
cryst system	monoclinic	tetragonal
space group	<i>P</i> 2 ₁ / <i>c</i>	<i>P</i> 4 ₂ / <i>mmc</i>
<i>a</i> , Å	12.643(4)	12.105(2)
<i>b</i> , Å	16.444(5)	12.105(2)
<i>c</i> , Å	18.445(5)	17.320(5)
β, deg	91.57(2)	90
<i>V</i> , Å ³	3833(2)	2537.9(9)
<i>Z</i>	4	2
<i>D</i> _{calcd} , g cm ⁻³	1.146	1.062
abs coeff, mm ⁻¹	0.800	0.459
cryst dmns, mm	0.20 × 0.10 × 0.30	0.30 × 0.15 × 0.10
scan type	ω/2θ	θ/2θ
scan sp in ω: min, max	6.0, 30.0	6.0, 30.0
2θ range, deg	3.0–44.0	3.0–42.0
<i>T</i> , K	230	220
decay, %	0	0
data collcd	5191	2935
obsd reflns, <i>F</i> > 6.0σ(<i>F</i>)	2807	706 [<i>F</i> > 4.0σ(<i>F</i>)]
params refined	343	88
GOF	1.26	1.12
Δρ(max, min), e/Å ³	0.44, -0.29	0.33, -0.20
<i>R</i> ^b	0.046	0.071
w <i>R</i>	0.052 ^c	w <i>R</i> ₂ = 0.185 ^d

^a Graphite monochromatized Mo Kα radiation, λ = 0.710 73 Å. ^b $R = \sum ||F_o| - |F_c|| / \sum |F_o|$; w*R* = $[\sum w(F_o - F_c)^2 / \sum w(F_o)^2]^{1/2}$. ^c $w = 1/[\sigma^2(F_o) + 0.0005(F_o)^2]$. ^d $w = 1/[\sigma^2(F_o^2) + (0.1324P)^2 + 0.4848P]$, where $P = (F_o^2 + 2F_c^2)/3$.

SHELXL 93.¹⁵ All other structures were refined using SHELXL-Plus.¹⁴ Weighted w*R* and goodness of fit were based on *F*², and the conventional *R*-factor was based on *F*, with *F* set equal to zero for negative *F*². While *F* > 4.0σ(*F*) was used for the *R*-factor calculation, for refinement, *F* > 6.0σ(*F*) was chosen. Scattering factors, with corrections for the anomalous dispersions of Co, Mn, and lanthanide metals, were taken from ref 16. Full-matrix least-squares refinements were performed

(15) Sheldrick, G. M. Shelxl93, program for the refinement of Crystal Structures. Univ. of Göttingen, Germany, 1993.

(16) *International Tables For X-ray Crystallography*; Kynoch press: Birmingham, U.K., 1974; Vol. IV.

for all structures. All non-H atoms of **3** were anisotropically refined. The benzene molecules of crystallization in **1–5** were disordered. Therefore, in the structures of **1**, **2**, **4**, and **5**, these molecules were converted into regular hexagons in the final stages of refinement. However, in the structure of **3**, the C atoms of the disordered benzenes were constrained during the final refinement and its H atoms were generated. The disordered THF molecules of **2–5** were all elastically restrained. In compound **4**, only the Dy, Si, O, and methyl-C atoms were anisotropically refined. The unit cell of **7** consisted of an anionic full-sandwich cobaltacarborane, having a well-separated Li(TMEDA)₂⁺ counter ion, plus a solvating benzene. The Co atom was located at the crystallographic *mmm* center, while the Li was positioned at $\bar{4}2m$. The anion was statistically disordered; the occupancy factors were as follows: Co and Li, 0.125; B(5) and B(7), 0.25; Si, C(2), B(4), C(12), N(21), and C(22), 0.50. All of the carborane-cage H atoms of **1–3** and **5–7** were located in Δ*F* maps. The cage-H's of **3** were freely refined, and their isotropic displacement parameters were refined as common free variables.¹¹ No attempts were made to locate the H atoms in the structure of **4**. The methyl and methylene-H's of **1–3** and **5–7** were placed using a riding model. The final values of *R* and weighted w*R* are listed in Tables 3 and 4. For all structures, $R = \sum (|F_o| - |F_c|) / \sum |F_o|$. For **1**, **2**, and **4–6**, w*R* = $[\sum w|F_o| - |F_c|]^2 / \sum w|F_o|^2]^{1/2}$, with $w = [\sigma^2(F) + 0.001(F)^2]^{-1}$. For **3**, the weight had the form $w = [1/\sigma^2(F^2) + 0.0410P^2 + 14.4051P]$, while, for **7**, $w = [1/\sigma^2(F_o^2) + 0.1324P^2 + 0.4848P]$, where $P = (F_o^2 + 2F_c^2)/3$. The atomic coordinates are given in Tables 5 and 6, while selected interatomic distances and angles are listed in Tables 7 and 8, respectively.

Results and Discussion

Synthesis. The reaction between *closo-exo*-4,5-Li-(THF)₂-1-Li(THF)₂-2,3-(SiMe₃)₂-2,3-C₂B₄H₄ and anhydrous LnCl₃ (Ln = Sm, Gd, Tb, Dy, Ho) in a molar ratio of 2:1 in dry benzene (C₆H₆), followed by extraction and crystallization of the product from benzene solution, yielded the half-sandwich paramagnetic species { $[\eta^5$ -1-Ln-2,3-(SiMe₃)₂-2,3-C₂B₄H₄]₃[(μ₂-1-Li-2,3-(SiMe₃)₂-2,3-C₂B₄H₄]₃(μ₃-OMe)][(μ₂-Li(C₄H₈O)]₃(μ₃-O)}·1.5C₆H₆ (Ln = Sm (**1**), Gd (**2**), Tb (**3**), Dy (**4**), Ho (**5**)) in yields of 59%,

Table 5. Atomic Coordinates ($\times 10^4$) and Equivalent Isotropic Displacement Coefficients ($\text{\AA}^2 \times 10^3$) for 1, 2, 4, and 5a

	<i>x</i>	<i>y</i>	<i>z</i>	<i>U</i> (eq) ^b		<i>x</i>	<i>y</i>	<i>z</i>	<i>U</i> (eq) ^b
Compound 1									
Sm(1)	1232(1)	4207(2579	39(1)	C(72)	-1579(8)	5335(3401	89(6)
Sm(2)	3304(1)	3103(1)	1671(1)	37(1)	C(73)	-403(9)	5755(10)	4207(4)	110(8)
Sm(3)	3476(1)	2956(1)	3266(1)	34(1)	C(74)	-1969(9)	6039(10)	2008(6)	116(8)
Li(1)	2311(13)	5727(11)	1731(7)	62(8)	C(75)	-602(8)	5772(8)	1129(5)	94(7)
Li(2)	4740(12)	4322(11)	2425(7)	63(8)	C(76)	-1250(9)	7429(7)	1764(5)	100(7)
Li(3)	2494(11)	5524(11)	3418(7)	59(8)	C(77)	-1060(11)	2633(12)	583(7)	164(11)
Li(4)	1493(11)	2138(11)	1950(6)	53(8)	C(78)	-800(10)	1771(9)	1686(7)	133(9)
Li(5)	3289(10)	1132(10)	2404(6)	49(7)	C(79)	-1614(8)	3661(9)	1606(6)	119(8)
Li(6)	1719(11)	1934(11)	3188(7)	60(8)	C(80)	1104(13)	1929(10)	-182(5)	147(12)
Si(1)	-887(2)	6000(2)	3488(1)	71(1)	C(81)	2714(10)	849(9)	454(6)	127(9)
Si(2)	-960(2)	6252(2)	1843(1)	73(1)	C(82)	952(10)	635(8)	693(5)	108(8)
Si(3)	-734(2)	2687(2)	1323(2)	90(2)	C(83)	2290(12)	4753(9)	-140(6)	153(11)
Si(4)	1449(3)	1450(2)	502(1)	79(2)	C(84)	4128(12)	4038(11)	-532(5)	143(12)
Si(5)	3313(3)	3884(2)	-34(1)	79(2)	C(85)	3132(10)	2904(8)	-247(4)	102(8)
Si(6)	5630(2)	2604(2)	646(1)	79(2)	C(86)	6267(10)	3215(10)	323(7)	142(10)
Si(7)	5034(3)	-545(2)	1582(1)	76(2)	C(87)	6348(8)	1890(9)	1231(5)	102(7)
Si(8)	4972(3)	-561(2)	3211(2)	77(2)	C(88)	5474(10)	1880(9)	131(6)	118(8)
Si(9)	6042(2)	2216(2)	4010(2)	78(2)	C(89)	5272(9)	-202(8)	891(5)	104(8)
Si(10)	3962(2)	3435(2)	4967(1)	68(2)	C(90)	6116(9)	-1384(9)	1803(6)	143(9)
Si(11)	1720(3)	1270(2)	4692(1)	77(2)	C(91)	4209(10)	-1051(8)	1507(5)	112(8)
Si(12)	-474(3)	2485(3)	3907(2)	94(2)	C(92)	4362(10)	-177(8)	3883(5)	106(8)
O(10)	2697(3)	3526(3)	2503(2)	36(2)	C(93)	6196(10)	-945(9)	3331(6)	126(8)
C(11)	64(6)	5742(6)	2966(4)	50(4)	C(94)	4611(10)	-1454(8)	3012(5)	104(7)
C(12)	13(6)	5809(5)	2340(4)	51(5)	C(95)	5993(10)	1210(8)	4241(8)	156(10)
B(13)	931(8)	5785(7)	2079(5)	52(5)	C(96)	6591(9)	2606(10)	4568(6)	120(8)
B(14)	1619(8)	5699(7)	2596(5)	52(5)	C(97)	6773(8)	1924(9)	3369(5)	129(8)
B(15)	1019(9)	5651(7)	3163(5)	51(5)	C(98)	4499(12)	2350(11)	5279(6)	167(12)
B(16)	471(8)	6449(8)	2670(5)	61(6)	C(99)	2746(9)	3758(10)	5106(5)	124(10)
C(21)	393(7)	2753(6)	1385(4)	52(5)	C(100)	4377(12)	4185(11)	5316(5)	140(12)
C(22)	1244(7)	2267(6)	1073(4)	57(5)	C(101)	2734(9)	1201(8)	5074(5)	95(7)
B(23)	1969(8)	2650(7)	1156(5)	51(5)	C(102)	1860(10)	197(7)	4437(5)	104(8)
B(24)	1500(8)	3494(7)	1552(4)	51(6)	C(103)	768(10)	1659(10)	5218(5)	120(9)
B(25)	500(8)	3483(8)	1723(5)	51(5)	C(104)	-1118(8)	3222(9)	4459(6)	113(8)
B(26)	840(9)	3328(8)	999(5)	59(6)	C(105)	-1062(9)	2831(10)	3212(7)	136(10)
C(31)	3657(7)	3854(6)	703(4)	52(5)	C(106)	-428(11)	1366(10)	4039(7)	143(11)
C(32)	4560(7)	3360(6)	967(4)	53(5)	O(110)	2076(4)	1372(4)	2518(2)	48(3)
B(33)	4662(8)	3736(7)	1547(5)	51(6)	C(111)	1863(9)	623(8)	2543(5)	95(7)
B(34)	3711(8)	4580(7)	1646(4)	45(5)	O(121)	2256(7)	6826(5)	1499(4)	94(4)
B(35)	3082(8)	4611(8)	1101(5)	51(6)	C(122)	1775(21)	7603(17)	1705(11)	332(27)
B(36)	4247(9)	4444(8)	963(5)	58(6)	C(123)	1783(20)	8210(13)	1376(13)	271(23)
C(41)	4617(6)	373(5)	2080(4)	51(4)	C(124)	2334(21)	7952(15)	989(10)	233(22)
C(42)	4615(6)	354(6)	2695(4)	52(5)	C(125)	2372(26)	7163(16)	1060(11)	474(49)
B(43)	4422(7)	1251(7)	2944(5)	46(5)	O(126)	5448(6)	4976(6)	2436(3)	92(5)
B(44)	4339(7)	1910(7)	2394(5)	46(5)	C(127)	5546(12)	5468(10)	2004(6)	128(11)
B(45)	4382(8)	1329(7)	1846(5)	46(5)	C(128)	5500(13)	6300(10)	2237(7)	147(12)
B(46)	5242(8)	866(7)	2367(5)	56(5)	C(129)	5738(12)	6079(10)	2816(7)	122(10)
C(51)	4924(6)	3050(6)	3819(4)	44(4)	C(130)	5812(12)	5238(12)	2891(6)	135(12)
C(52)	4132(6)	3492(6)	4195(4)	44(4)	O(131)	2453(6)	6597(5)	3669(4)	85(4)
B(53)	3460(8)	4332(7)	3904(4)	46(5)	C(132)	1693(14)	7383(12)	3683(11)	220(17)
B(54)	3926(8)	4403(7)	3280(4)	44(5)	C(133)	2122(21)	7992(12)	3806(13)	334(31)
B(55)	4872(7)	3534(7)	3249(4)	39(5)	C(134)	2823(25)	7564(23)	3658(17)	548(55)
B(56)	4645(8)	4128(8)	3890(5)	52(6)	C(135)	3020(15)	6806(12)	3919(11)	221(16)
C(61)	1541(7)	2057(6)	4098(4)	53(5)	C(141)	1963(12)	202(14)	7306(19)	300
C(62)	689(7)	2519(6)	3799(4)	55(5)	C(142)	1611	210	7844	300
B(63)	749(8)	3266(8)	3448(5)	56(6)	C(143)	686	455	7926	300
B(64)	1739(7)	3284(7)	3556(5)	47(5)	C(144)	113	693	7469	300
B(65)	2262(8)	2445(7)	3956(4)	45(5)	C(145)	465	685	6930	300
B(66)	1142(8)	3122(8)	4155(4)	55(6)	C(146)	1319	440	6849	300
C(71)	-1619(9)	7139(7)	3424(6)	112(7)					
Compound 2									
Gd(1)	1267(1)	4214(1)	2576(1)	37(1)	Si(12)	-462(3)	2516(3)	3885(2)	87(2)
Gd(2)	3333(1)	3111(1)	1682(1)	35(1)	O(10)	2734(4)	3536(4)	2513(3)	35(3)
Gd(3)	3488(1)	2972(1)	3262(1)	32(1)	C(11)	77(8)	5727(7)	2963(5)	51(6)
Li(1)	2294(15)	5728(14)	1723(9)	63(10)	C(12)	27(8)	5808(7)	2326(5)	47(5)
Li(2)	4742(15)	4337(14)	2423(8)	64(11)	B(13)	960(9)	5770(8)	2072(5)	40(6)
Li(3)	2475(14)	5526(12)	3430(9)	60(9)	B(14)	1613(9)	5719(8)	2586(6)	51(6)
Li(4)	1505(14)	2159(16)	1954(9)	70(11)	B(15)	1029(9)	5637(8)	3173(6)	46(6)
Li(5)	3295(13)	1154(12)	2422(7)	45(8)	B(16)	467(10)	6452(9)	2659(6)	58(7)
Li(6)	1750(14)	1947(13)	3179(9)	60(10)	C(21)	422(8)	2775(7)	1389(5)	51(6)
Si(1)	-876(2)	5991(3)	3482(2)	67(2)	C(22)	1278(8)	2277(7)	1073(5)	49(6)
Si(2)	-940(3)	6252(2)	1832(2)	68(2)	B(23)	2004(10)	2662(9)	1171(6)	51(7)
Si(3)	-699(3)	2712(3)	1304(2)	86(2)	B(24)	1539(9)	3505(8)	1555(5)	44(6)
Si(4)	1512(3)	1448(3)	513(2)	77(2)	B(25)	531(8)	3505(9)	1724(6)	44(6)
Si(5)	3360(3)	3849(3)	-30(2)	75(2)	B(26)	879(10)	3387(10)	1001(6)	58(7)
Si(6)	5675(3)	2578(3)	659(2)	78(2)	C(31)	3703(8)	3827(7)	722(4)	45(6)
Si(7)	5091(3)	-539(3)	1594(2)	75(2)	C(32)	4588(7)	3340(7)	984(5)	46(6)
Si(8)	4990(3)	-542(2)	3219(2)	75(2)	B(33)	4683(9)	3744(9)	1546(6)	48(7)
Si(9)	6054(3)	2213(3)	4012(2)	74(2)	B(34)	3766(9)	4561(8)	1641(5)	41(6)
Si(10)	3961(3)	3436(3)	4968(1)	65(2)	B(35)	3127(9)	4578(9)	1112(5)	47(7)
Si(11)	1720(3)	1300(3)	4686(2)	72(2)	B(36)	4269(11)	4423(10)	970(6)	59(7)

Table 5. (Continued)

	<i>x</i>	<i>y</i>	<i>z</i>	<i>U</i> (eq) ^b		<i>x</i>	<i>y</i>	<i>z</i>	<i>U</i> (eq) ^b	
Compound 2										
C(41)	4626(7)	418(7)	2087(5)	48(5)	C(92)	4378(10)	-147(9)	3892(5)	94(8)	
C(42)	4628(8)	379(7)	2711(5)	48(6)	C(93)	6180(11)	-930(10)	3334(7)	128(10)	
B(43)	4421(8)	1286(8)	2945(5)	37(6)	C(94)	4665(13)	-1423(10)	3032(7)	122(10)	
B(44)	4345(9)	1902(9)	2403(6)	49(6)	C(95)	6028(11)	1201(9)	4231(8)	137(11)	
B(45)	4422(8)	1324(9)	1858(6)	43(6)	C(96)	6596(10)	2616(12)	4539(8)	132(11)	
B(46)	5243(9)	899(9)	2392(6)	50(6)	C(97)	6784(10)	1938(12)	3374(7)	135(10)	
C(51)	4945(7)	3036(7)	3824(4)	37(5)	C(98)	4477(13)	2386(12)	5293(7)	150(13)	
C(52)	4131(8)	3489(7)	4184(4)	44(6)	C(99)	2731(9)	3765(10)	5120(5)	90(8)	
B(53)	3471(9)	4327(8)	3903(5)	38(6)	C(100)	4391(14)	4177(13)	5328(6)	153(16)	
B(54)	3939(9)	4404(8)	3295(5)	38(6)	C(101)	2743(10)	1214(9)	5084(6)	97(8)	
B(55)	4874(9)	3541(9)	3260(6)	46(7)	C(102)	1884(11)	214(9)	4433(7)	97(8)	
B(56)	4642(10)	4130(9)	3892(6)	53(7)	C(103)	772(11)	1701(11)	5213(6)	110(10)	
C(61)	1561(8)	2062(8)	4087(4)	51(6)	C(104)	-1134(10)	3259(11)	4412(8)	131(11)	
C(62)	693(8)	2545(8)	3771(5)	54(6)	C(105)	-1047(11)	2864(12)	3231(7)	130(11)	
B(63)	765(9)	3287(9)	3425(6)	49(7)	C(106)	-419(11)	1398(11)	4010(8)	131(12)	
B(64)	1756(9)	3298(8)	3562(5)	41(6)	O(110)	2107(5)	1372(5)	2516(3)	44(3)	
B(65)	2278(9)	2472(8)	3941(5)	47(6)	C(111)	1882(11)	629(10)	2523(6)	101(9)	
B(66)	1177(10)	3138(9)	4132(6)	55(7)	O(121)	2282(7)	6815(5)	1503(4)	106(6)	
C(71)	-1617(10)	7126(9)	3437(7)	112(9)	C(122)	1667(11)	7509(9)	1691(9)	348(24)	
C(72)	-1554(9)	5319(9)	3401(6)	82(7)	C(123)	1942(16)	8173(11)	1547(9)	295(18)	
C(73)	-421(9)	5790(11)	4186(5)	100(9)	C(124)	2355(15)	7886(13)	1034(8)	270(16)	
C(74)	-1986(10)	6070(11)	2020(7)	105(9)	C(125)	2799(11)	7026(10)	1158(8)	272(17)	
C(75)	-585(9)	5773(8)	1149(5)	82(7)	O(126)	5459(7)	4984(7)	2434(4)	90(6)	
C(76)	-1226(10)	7430(8)	1754(7)	98(8)	C(127)	5604(13)	5472(13)	1996(7)	114(11)	
C(77)	-1001(12)	2650(13)	569(8)	149(13)	C(128)	5522(18)	6259(14)	2232(10)	169(17)	
C(78)	-791(12)	1792(11)	1663(8)	128(11)	C(129)	5727(14)	6084(12)	2823(9)	122(12)	
C(79)	-1588(9)	3679(10)	1575(7)	108(9)	C(130)	5847(14)	5226(14)	2909(8)	132(14)	
C(80)	1194(14)	1921(10)	-186(6)	133(13)	O(131)	2456(7)	6591(6)	3673(4)	82(5)	
C(81)	2752(11)	839(10)	457(7)	116(10)	C(132)	1762(23)	7296(17)	3689(14)	276(30)	
C(82)	1025(12)	639(9)	681(6)	106(10)	C(133)	1963(23)	7941(24)	3748(18)	349(38)	
C(83)	2306(12)	4736(12)	-131(7)	140(13)	C(134)	2797(27)	7749(19)	3890(13)	262(35)	
C(84)	4207(12)	3991(12)	-519(5)	119(12)	C(135)	3099(15)	6870(17)	3848(12)	221(21)	
C(85)	3161(12)	2886(10)	-235(5)	103(10)	C(141)	1962(13)	201(15)	7335(23)	300	
C(86)	6318(12)	3221(12)	379(8)	140(12)	C(142)	1597	219	7871	300	
C(87)	6408(9)	1857(9)	1235(6)	97(8)	C(143)	669	461	7946	300	
C(88)	5553(11)	1846(11)	137(7)	119(10)	C(144)	106	686	7484	300	
C(89)	5328(11)	-208(9)	901(6)	104(9)	C(145)	472	668	6947	300	
C(90)	6152(10)	-1376(10)	1831(7)	126(9)	C(146)	1399	426	6873	300	
C(91)	4258(12)	-1055(10)	1519(6)	106(10)						
Compound 4										
Dy(1)	1321(1)	4201(1)	2552(1)	39(1)	C(42)	4643(13)	399(12)	2743(8)	47(5)	
Dy(2)	3392(1)	3092(1)	1694(1)	35(1)	B(43)	4430(16)	1278(15)	2995(10)	46(6)	
Dy(3)	3489(1)	2988(1)	3266(1)	34(1)	B(44)	4368(14)	1944(14)	2420(9)	35(6)	
Li(1)	2359(31)	5659(29)	1700(19)	84(13)	B(45)	4445(15)	1313(14)	1838(9)	40(6)	
Li(2)	4777(23)	4304(22)	2450(14)	50(9)	B(46)	5254(16)	904(15)	2435(10)	46(6)	
Li(3)	2473(29)	5497(27)	3457(18)	77(12)	C(51)	4927(14)	3047(13)	3839(9)	52(6)	
Li(4)	1581(27)	2110(26)	1957(17)	69(11)	C(52)	4105(14)	3505(13)	4184(8)	50(6)	
Li(5)	3334(25)	1165(24)	2393(16)	61(10)	B(53)	3454(15)	4349(14)	3919(9)	37(6)	
Li(6)	1772(23)	1931(22)	3138(14)	52(9)	B(54)	3944(15)	4417(14)	3296(9)	40(6)	
Si(1)	-843(4)	5978(4)	3448(3)	68(3)	B(55)	4892(17)	3529(16)	3255(11)	54(7)	
Si(2)	-883(5)	6205(4)	1782(3)	71(3)	B(56)	4649(18)	4094(17)	3923(11)	59(7)	
Si(3)	-619(5)	2699(5)	1218(4)	87(4)	C(61)	1554(13)	2100(12)	4058(8)	43(5)	
Si(4)	1657(5)	1380(5)	491(3)	74(4)	C(62)	700(14)	2550(14)	3741(9)	58(6)	
Si(5)	3469(6)	3771(5)	-25(3)	73(4)	B(63)	803(20)	3295(19)	3362(12)	72(8)	
Si(6)	5779(5)	2498(5)	704(3)	75(4)	B(64)	1767(15)	3343(14)	3542(9)	39(6)	
Si(7)	5149(5)	-564(4)	1622(3)	74(3)	B(65)	2258(16)	2467(16)	3947(10)	49(7)	
Si(8)	4983(5)	-525(4)	3244(3)	67(3)	B(66)	1137(18)	3193(16)	4100(11)	56(7)	
Si(9)	6027(5)	2211(5)	4048(3)	84(4)	C(71)	-1558(21)	7187(19)	3393(14)	131(17)	
Si(10)	3904(5)	3444(5)	4986(3)	73(4)	C(72)	-1512(17)	5289(17)	3347(11)	87(14)	
Si(11)	1673(5)	1338(4)	4671(3)	72(4)	C(73)	-367(21)	5782(19)	4160(12)	111(16)	
Si(12)	-465(5)	2522(6)	3812(4)	93(4)	C(74)	-1953(18)	6056(20)	2001(13)	108(16)	
O(10)	2777(7)	3512(7)	2488(4)	27(3)	C(75)	-520(16)	5707(16)	1091(10)	82(12)	
C(11)	103(14)	5692(13)	2921(9)	51(6)	C(76)	-1171(21)	7394(17)	1715(12)	113(15)	
C(12)	114(13)	5773(12)	2292(8)	43(5)	C(77)	-829(22)	2682(25)	444(14)	138(22)	
B(13)	1023(18)	5736(17)	2035(11)	59(7)	C(78)	-744(29)	1763(24)	1597(16)	159(27)	
B(14)	1662(17)	5649(16)	2597(10)	53(7)	C(79)	-1569(17)	3666(21)	1529(14)	111(17)	
B(15)	1068(16)	5598(15)	3149(10)	47(6)	C(80)	1354(30)	1866(24)	-227(12)	158(26)	
B(16)	514(19)	6444(18)	2649(12)	66(8)	C(81)	2891(21)	802(20)	468(13)	119(18)	
C(21)	525(15)	2730(14)	1336(10)	66(7)	C(82)	1137(29)	594(20)	641(13)	146(25)	
C(22)	1414(14)	2230(13)	1043(8)	51(6)	C(83)	2407(19)	4696(21)	-155(11)	104(17)	
B(23)	2132(18)	2634(16)	1145(11)	56(7)	C(84)	4367(23)	3914(22)	-508(11)	115(19)	
B(24)	1656(16)	3489(15)	1523(10)	45(6)	C(85)	3253(21)	2813(19)	-236(10)	96(17)	
B(25)	600(16)	3482(15)	1687(10)	44(6)	C(86)	6421(18)	3139(20)	429(12)	100(16)	
B(26)	1009(18)	3367(17)	968(11)	60(7)	C(87)	6428(18)	1807(20)	1258(12)	102(16)	
C(31)	3789(14)	3781(13)	736(8)	52(6)	C(88)	5641(20)	1759(19)	144(12)	106(16)	
C(32)	4679(14)	3279(13)	1009(9)	53(6)	C(89)	5436(20)	-228(18)	896(11)	98(15)	
B(33)	4772(16)	3683(15)	1563(10)	45(6)	C(90)	6237(21)	-1384(17)	1888(14)	119(16)	
B(34)	3844(15)	4516(14)	1653(9)	39(6)	C(91)	4372(22)	-1133(17)	1546(12)	105(17)	
B(35)	3198(16)	4504(15)	1105(10)	43(6)	C(92)	4289(21)	-82(15)	3935(10)	95(15)	
B(36)	4329(18)	4364(17)	992(11)	58(7)	C(93)	6136(18)	-969(18)	3374(12)	98(14)	
C(41)	4685(14)	410(13)	2100(9)	52(6)	C(94)	4628(28)	-1427(19)	3024(12)	135(22)	

Table 5. (Continued)

	<i>x</i>	<i>y</i>	<i>z</i>	<i>U</i> (eq) ^b		<i>x</i>	<i>y</i>	<i>z</i>	<i>U</i> (eq) ^b
Compound 4									
C(95)	6055(22)	1118(18)	4238(16)	127(18)	C(125)	2978(17)	6973(22)	1188(15)	236(24)
C(96)	6572(21)	2631(24)	4624(12)	123(20)	O(126)	5533(13)	4940(12)	2458(6)	95(11)
C(97)	6846(20)	1850(30)	3427(15)	185(26)	C(127)	5705(18)	5384(18)	1977(12)	89(8)
C(98)	4476(23)	2328(23)	5313(14)	146(20)	C(128)	5548(22)	6273(21)	2232(14)	117(11)
C(99)	2656(21)	3813(23)	5116(11)	118(19)	C(129)	5734(24)	6070(23)	2867(15)	130(12)
C(100)	4334(26)	4208(25)	5339(12)	143(24)	C(130)	5904(19)	5181(19)	2967(12)	92(9)
C(101)	2735(19)	1238(18)	5077(10)	90(15)	O(131)	2476(12)	6609(10)	3683(7)	90(9)
C(102)	1791(22)	211(17)	4405(12)	105(17)	C(132)	1650(14)	7258(20)	3788(14)	195(19)
C(103)	714(21)	1729(19)	5204(12)	109(16)	C(133)	1796(31)	8075(18)	3744(18)	290(31)
C(104)	-1182(19)	3218(21)	4401(13)	116(17)	C(134)	2715(34)	7803(24)	3977(17)	299(32)
C(105)	-1082(21)	2887(27)	3124(14)	146(23)	C(135)	3138(16)	6949(21)	3711(15)	220(22)
C(106)	-435(18)	1385(18)	3951(14)	109(17)	C(141)	1266(127)	320(41)	7961(20)	400
O(110)	2128(9)	1352(9)	2492(5)	50(6)	C(142)	394	549	7756	400
C(111)	1873(22)	582(20)	2488(12)	106(18)	C(143)	236	680	7181	400
O(121)	2335(13)	6776(10)	1489(8)	98(9)	C(144)	950	582	6810	400
C(122)	1612(18)	7531(19)	1599(17)	290(32)	C(145)	1822	354	7015	400
C(123)	1924(33)	8240(17)	1475(20)	326(37)	C(146)	1980	223	7590	400
C(124)	2533(32)	7869(27)	990(16)	233(24)					
Compound 5									
Ho(1)	1331(1)	4192(1)	2552(1)	32(1)	C(72)	-1517(10)	5290(10)	3360(7)	83(8)
Ho(2)	3400(1)	3089(1)	1697(1)	29(1)	C(73)	-395(10)	5770(11)	4167(6)	88(9)
Ho(3)	3493(1)	2986(1)	3262(1)	28(1)	C(74)	-1936(9)	5998(11)	1975(7)	92(9)
Li(1)	2390(12)	5643(13)	1710(9)	44(8)	C(75)	-532(9)	5703(9)	1077(5)	64(7)
Li(2)	4825(16)	4254(17)	2457(10)	60(11)	C(76)	-1172(10)	7350(9)	1727(7)	82(8)
Li(3)	2498(15)	5499(15)	3427(10)	59(10)	C(77)	-817(12)	2670(13)	446(8)	125(12)
Li(4)	1604(17)	2140(15)	1945(11)	70(12)	C(78)	-722(13)	1781(12)	1551(9)	131(13)
Li(5)	3337(15)	1138(13)	2397(10)	53(9)	C(79)	-1505(9)	3650(11)	1489(8)	97(9)
Li(6)	1795(15)	1931(15)	3164(9)	54(10)	C(80)	1405(14)	1814(11)	-234(6)	108(12)
Si(1)	-843(3)	5954(3)	3445(2)	59(2)	C(81)	2915(12)	772(10)	495(7)	105(10)
Si(2)	-882(3)	6187(3)	1786(2)	60(2)	C(82)	1171(14)	564(12)	647(8)	119(12)
Si(3)	-595(3)	2690(3)	1195(2)	76(2)	C(83)	2433(11)	4639(11)	-166(7)	104(11)
Si(4)	1689(3)	1364(3)	492(2)	67(2)	C(84)	4357(12)	3893(12)	-509(6)	100(11)
Si(5)	3495(3)	3753(3)	-28(2)	60(2)	C(85)	3283(12)	2783(11)	-244(6)	91(10)
Si(6)	5785(3)	2495(3)	709(2)	62(2)	C(86)	6427(10)	3135(11)	427(7)	95(10)
Si(7)	5169(3)	-572(3)	1626(2)	61(2)	C(87)	6455(10)	1800(10)	1271(7)	87(9)
Si(8)	4964(3)	-520(2)	3251(2)	60(2)	C(88)	5648(12)	1770(11)	141(7)	98(10)
Si(9)	6034(3)	2199(3)	4045(2)	66(2)	C(89)	5428(12)	-240(10)	929(7)	98(10)
Si(10)	3916(3)	3432(3)	4988(2)	61(2)	C(90)	6230(11)	-1386(10)	1904(7)	102(9)
Si(11)	1670(3)	1350(3)	4671(2)	58(2)	C(91)	4369(11)	-1116(9)	1523(7)	84(9)
Si(12)	-450(3)	2498(3)	3790(2)	75(2)	C(92)	4340(12)	-140(10)	3929(6)	94(9)
O(10)	2781(4)	3521(4)	2508(3)	26(3)	C(93)	6151(10)	-948(10)	3406(7)	96(9)
C(11)	113(8)	5674(8)	2929(5)	43(5)	C(94)	4606(12)	-1403(9)	3040(7)	98(10)
C(12)	95(8)	5757(7)	2291(5)	40(5)	C(95)	5995(12)	1171(10)	4261(9)	121(11)
B(13)	1029(10)	5711(9)	2063(6)	44(6)	C(96)	6547(11)	2614(12)	4635(8)	114(11)
B(14)	1662(9)	5661(9)	2580(6)	42(6)	C(97)	6813(10)	1922(12)	3428(8)	119(11)
B(15)	1059(10)	5598(9)	3142(6)	43(6)	C(98)	4446(14)	2359(12)	5319(7)	129(13)
B(16)	520(10)	6405(9)	2633(7)	49(7)	C(99)	2695(10)	3790(11)	5132(6)	85(9)
C(21)	530(8)	2736(8)	1335(5)	42(5)	C(100)	4342(13)	4168(13)	5366(6)	118(13)
C(22)	1430(9)	2226(8)	1039(5)	46(6)	C(101)	2680(11)	1246(9)	5081(6)	82(8)
B(23)	2179(11)	2595(10)	1152(6)	50(7)	C(102)	1838(12)	232(9)	4432(7)	92(9)
B(24)	1621(10)	3482(10)	1538(6)	47(7)	C(103)	706(12)	1753(12)	5178(6)	102(11)
B(25)	625(10)	3477(9)	1682(6)	40(6)	C(104)	-1154(10)	3249(11)	4345(7)	107(10)
B(26)	1023(10)	3318(9)	961(7)	47(7)	C(105)	-1005(11)	2833(12)	3103(8)	109(11)
C(31)	3809(9)	3750(8)	727(5)	42(6)	C(106)	-431(11)	1403(11)	3916(8)	104(11)
C(32)	4681(9)	3261(8)	1009(5)	40(6)	O(110)	2136(5)	1338(5)	2486(3)	40(4)
B(33)	4761(9)	3662(9)	1587(6)	36(6)	C(111)	1896(11)	559(12)	2513(7)	109(11)
B(34)	3820(10)	4515(9)	1673(6)	43(7)	O(121)	2371(8)	6775(6)	1510(5)	96(6)
B(35)	3202(10)	4542(9)	1116(6)	41(7)	C(122)	1686(11)	7485(10)	1613(11)	440(35)
B(36)	4369(10)	4345(10)	994(6)	47(7)	C(123)	1972(18)	8156(8)	1484(11)	319(22)
C(41)	4683(8)	398(8)	2101(5)	40(5)	C(124)	2581(17)	7797(12)	1042(11)	235(15)
C(42)	4626(8)	388(8)	2734(5)	42(5)	C(125)	2942(13)	6921(11)	1166(12)	240(16)
B(43)	4435(9)	1290(9)	2972(6)	38(6)	O(126)	5529(8)	4954(7)	2464(4)	84(6)
B(44)	4394(9)	1917(9)	2420(6)	41(6)	C(127)	5689(12)	5406(11)	2008(6)	86(10)
B(45)	4468(10)	1307(10)	1867(6)	43(7)	C(128)	5540(14)	6262(13)	2242(9)	119(13)
B(46)	5254(10)	902(9)	2437(6)	44(6)	C(129)	5749(14)	6103(12)	2869(8)	107(12)
C(51)	4907(8)	3030(8)	3841(5)	44(6)	C(130)	5874(13)	5221(13)	2949(7)	103(12)
C(52)	4099(8)	3486(7)	4207(5)	37(5)	O(131)	2435(7)	6625(5)	3689(5)	75(5)
B(53)	3469(9)	4317(9)	3919(5)	32(6)	C(132)	1674(8)	7281(10)	3740(14)	325(33)
B(54)	3951(10)	4393(10)	3314(6)	42(7)	C(133)	1884(15)	7954(9)	3956(11)	246(26)
B(55)	4881(10)	3517(8)	3273(6)	35(6)	C(134)	2744(16)	7774(12)	3726(13)	289(35)
B(56)	4645(10)	4111(10)	3926(6)	44(7)	C(135)	3112(8)	6878(11)	3719(15)	260(26)
C(61)	1548(8)	2086(8)	4051(4)	37(5)	C(141)	1974(16)	219(18)	7534(38)	350
C(62)	704(8)	2567(8)	3735(5)	47(6)	C(142)	1405	267	7994	350
B(63)	784(9)	3297(10)	3373(6)	43(6)	C(143)	483	491	7912	350
B(64)	1777(10)	3308(8)	3525(6)	36(6)	C(144)	131	667	7371	350
B(65)	2259(11)	2464(9)	3927(6)	42(7)	C(145)	700	618	6911	350
B(66)	1124(10)	3183(9)	4087(6)	44(7)	C(146)	1622	394	6993	350
C(71)	-1591(11)	7125(9)	3381(7)	95(9)					

^a For **3**, see ref 11. ^b Equivalent isotropic *U* defined as one-third of the trace of the orthogonalized U_{ij} tensor.

Table 6. Atomic Coordinates ($\times 10^4$) and Equivalent Isotropic Displacement Coefficients ($\text{\AA}^2 \times 10^3$) for **6 and **7****

	<i>x</i>	<i>y</i>	<i>z</i>	<i>U</i> (eq) ^a
Compound 6				
Mn(1)	2377(1)	-551(1)	6905(1)	29(1)
Mn(2)	2392(1)	176(1)	5614(1)	31(1)
Si(1)	4412(2)	-1556(2)	8302(1)	59(1)
Si(2)	3320(2)	-2647(1)	6545(1)	51(1)
Si(3)	286(2)	-1233(1)	8326(1)	51(1)
Si(4)	1664(2)	912(1)	8295(1)	48(1)
C(11)	3796(5)	-1094(4)	7458(3)	39(3)
C(12)	3454(5)	-1537(4)	6791(3)	35(2)
B(13)	3439(6)	-968(5)	6103(4)	36(3)
B(14)	3810(6)	-49(5)	6431(4)	40(3)
B(15)	3969(6)	-172(6)	7316(4)	45(3)
B(16)	4545(7)	-893(5)	6704(4)	43(3)
C(21)	958(5)	-668(4)	7580(3)	33(2)
C(22)	1406(4)	172(4)	7539(3)	30(2)
B(23)	1421(6)	496(5)	6732(4)	33(3)
B(24)	930(6)	-291(5)	6230(4)	35(3)
B(25)	684(6)	-1014(5)	6815(4)	38(3)
B(26)	274(6)	9(5)	7016(4)	36(3)
C(31)	3424(7)	-2007(5)	8904(4)	80(4)
C(32)	5176(7)	-794(6)	8834(5)	97(4)
C(33)	5381(7)	-2341(6)	8046(4)	102(5)
C(34)	3052(8)	-3364(5)	7307(4)	91(4)
C(35)	4553(6)	-2977(5)	6095(5)	84(4)
C(36)	2187(6)	-2747(4)	5898(4)	61(3)
C(37)	557(7)	-2334(5)	8213(5)	80(4)
C(38)	632(7)	-973(5)	9278(4)	86(4)
C(39)	-1160(6)	-1056(6)	8203(4)	84(4)
C(40)	2351(7)	1810(5)	7924(5)	81(4)
C(41)	377(6)	1247(5)	8656(4)	72(4)
C(42)	2564(6)	506(5)	9016(4)	80(4)
N(51)	2537(4)	-178(3)	4444(3)	32(2)
N(52)	2197(4)	1412(3)	5091(3)	37(2)
C(53)	2159(5)	531(4)	4014(3)	38(2)
C(54)	2567(6)	1311(4)	4339(3)	53(3)
C(55)	1875(5)	-885(4)	4250(3)	44(3)
C(56)	3642(5)	-367(4)	4267(3)	49(3)
C(57)	2833(6)	2057(4)	5456(4)	65(3)
C(58)	1082(6)	1678(4)	5075(4)	54(3)
Compound 7				
Co	0	5000	0	67(1)
Si	0	2521(2)	1133(2)	113(1)
Li	5000	5000	2500	114(12)
C(12)	551(9)	3551(7)	442(5)	75(3)
B(13)	1298(13)	4568(11)	739(8)	84(4)
B(14)	1774(14)	5000	0	114(6)
B(16)	1887(21)	3740(18)	0	88(6)
C(18)	1169(9)	1539(11)	1081(8)	264(8)
C(19)	0	3112(11)	2118(5)	248(12)
N(21)	5000	3711(9)	1721(7)	163(4)
C(22)	5000	4334(4)	995(8)	591(67)
C(23)	4010(12)	3021(13)	1788(10)	311(10)
C(31)	4494(20)	0	649(13)	231(19)
C(32)	3931(30)	0	0	229(23)

^a Equivalent isotropic *U* defined as one-third of the trace of the orthogonalized U_{ij} tensor.

58%, 49%, 52%, and 59%, respectively (see Experimental Section and Scheme 1). In addition to containing the reactant units of lithium, carborane, and lanthanide, each product also incorporated a methoxide and an oxide ion, as coordination centers for three lithium and three lanthanide atoms, respectively. The oxygen source for the oxyanions in the products was the THF solvent used in the preparation of the dilithiacarborane precursor; it was the only oxygen-containing substance in the synthetic scheme. The production of isostructural compounds from five independent syntheses with different lanthanide metals makes it unlikely that some chance oxygen-containing contaminant could be responsible for the course of the reactions. Since both *t*-BuLi and lanthanide compounds are known to degrade THF,^{17,18}

and other oxygen-containing compounds,¹⁹ and the THF-solvated dilithiacarboranes are known to decompose,^{13b} it is not possible to ascertain how, or when, the methoxide and oxide ions were formed. Attempts to react **1–5** with excess LnCl₃ proved unsuccessful, resulting in the full recovery of the excess lanthanide salt. Therefore, however they are formed, the oxide and methoxide ions seem to stabilize the clusters to the extent that the syntheses of the metal-lacarboranes are effectively terminated. The fact that the reaction of ErCl₃,⁹ and other LnCl₃ salts,²⁰ with the TMEDA-solvated dilithiacarborane, in the absence of THF, produced exclusively the bent-sandwich metallocarboranes, [Li(TMEDA)₂][1-Cl-1-(*μ*-Cl)-2,2',3,3'-(SiMe₃)₄-5,6-[*μ*-H]₂Li(TMEDA)]-4,4',5'-(*μ*-H)₃Li(TMEDA)]-1,1'-*commo*-Ln(2,3-C₂B₄H₄)₂], is further evidence of direct THF involvement in the synthesis of **1–5**.

The reaction of **1** with anhydrous CoCl₂ in dry benzene solution produced, in 57% yield, a dark-red crystalline solid identified as the ionic cobalt(III) sandwich complex Li(THF)₄{1,1'-*commo*-Co[2,3-(SiMe₃)₂-2,3-C₂B₄H₄]₂} (**7a**). Attempts to grow suitable crystals of **7a** for X-ray structure determination were unsuccessful. However, it was found that the THF molecules of solvation could be quantitatively replaced by TMEDA molecules to give the readily crystallizable complex **7**, Li(TMEDA)₂{1,1'-*commo*-Co[2,3-(SiMe₃)₂-2,3-C₂B₄H₄]₂}. A similar reaction of **2** with MnCl₂ in a dry benzene solution, followed by addition of TMEDA, gave the zwitterionic dinuclear manganese complex 4,4',5,5'-Mn(TMEDA)-1,1'-*commo*-Mn[2,3-(SiMe₃)₂-2,3-C₂B₄H₄]₂ (**6**) as a dark red crystalline solid in 70% yield (Scheme 1). These products are quite different from those obtained from the direct reaction of the dilithiacarborane with either MnCl₂ or CoCl₂. When MnCl₂ was reacted directly, the mixed-valence trinuclear butterfly cluster {[Li(THF)][Li(TMEDA)]₂}{*commo*-Mn₃[2,3-(SiMe₃)₂-2,3-C₂B₄H₄]₄} was obtained,²¹ while CoCl₂ yielded a mixed-valence complex composed of a paramagnetic trinuclear [Co₃Cl₅]⁺ cation and an anionic sandwich Co(III) carborane.²² Since **6** and **7** are simpler than the products from the direct reactions, compounds **1–5** may prove to be useful synthons for obtaining targeted carborane complexes of d-block elements that would otherwise be difficult to synthesize.

Crystal Structures. Compounds **1–7** were characterized by single-crystal X-ray diffraction. Tables 3–6 give the pertinent crystallographic information and atomic coordinates of the compounds, while Tables 7 and 8 list some selected bond distances and bond angles. A more complete set of distances and angles is available in the Supporting Information. Compounds **1–5** are all isostructural so that their structures, shown in Figures 1–5, present different views that illustrate different

(17) (a) Jung, M. E.; Blum, R. B. *Tetrahedron Lett.* **1977**, 3791. (b) Maercker, A.; Theysohn, W. *J. Liebig's Ann Chem.* **1971**, 70, 747. (c) Kamata, K.; Terashima, M. *Heterocycles* **1980**, 14, 205.

(18) Schumann, H.; Palamidis, E.; Loebel, J. *J. Organomet. Chem.* **1990**, 384, C49–52.

(19) Evans, W. J.; Grate, J. W.; Bloom, I.; Hunter, W. E.; Atwood, J. L. *J. Am. Chem. Soc.* **1985**, 107, 405.

(20) Hosmane, N. S.; Wang, Y.; Zhang, H.; Maguire, J. A.; McInnis, M.; Gray, T. G.; Collins, J. D.; Kremer, R. K.; Binder, H.; Waldh r, E.; Kaim, W. *Organometallics*, in press (Part 20 in the series).

(21) Oki, A. R.; Zhang, H.; Hosmane, N. S.; Ro, H.; Hatfield, W. J. *Am. Chem. Soc.* **1991**, 113, 8531.

(22) Hosmane, N. S.; Wang, Y.; Zhang, H.; Maguire, J. A.; Yang, J.; Kremer, R. K.; Waldh r, E.; Kaim, W. Unpublished results.

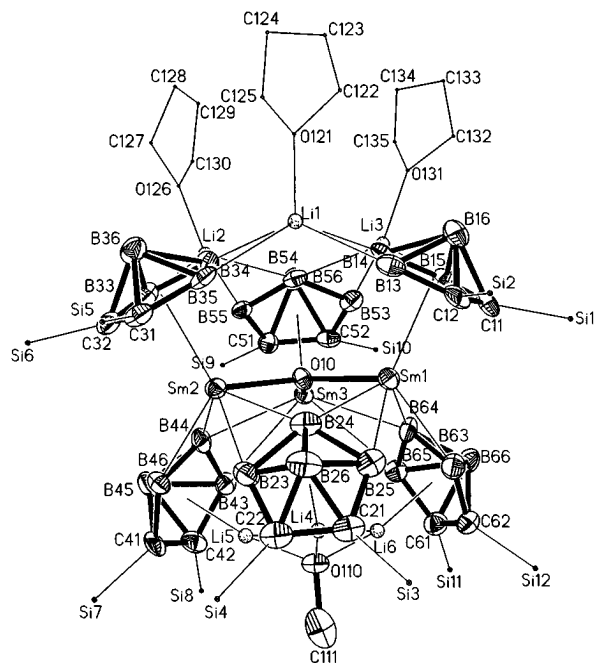


Figure 1. Perspective view of **1** showing the atom-numbering scheme with thermal ellipsoids drawn at the 25% probability level. The H atoms and the C atoms of the silyl groups are omitted for clarity.

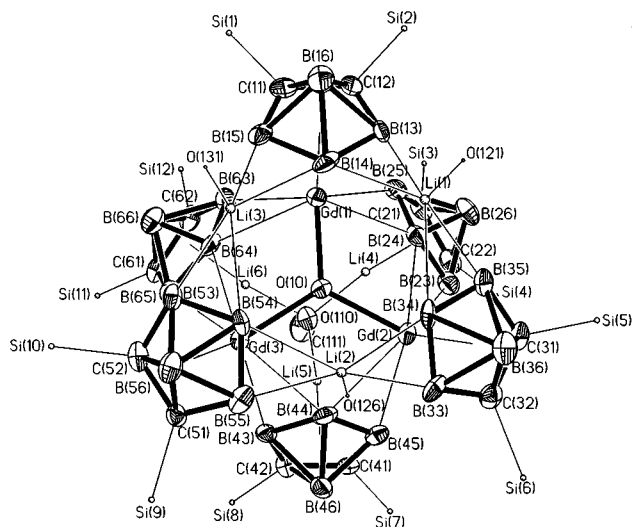


Figure 2. Perspective view of **2** showing the atom-numbering scheme with thermal ellipsoids drawn at the 25% probability level. The H atoms and the C atoms of the silyl groups, as well as the THF molecules, are omitted for clarity.

geometrical aspects. The structures of compounds **6** and **7** are shown in Figures 6 and 7, respectively.

Structures of 1–5. Figures 1–5 show that the lanthanacarboranes crystallize as clusters composed of three half-sandwich lithiacarboranes and three half-sandwich lanthanacarboranes arranged around a methoxide ion and an oxide ion, respectively. The Ln_3O geometry is that of a trigonal plane in which the three lanthanides equally surround the central oxide; the $\text{Ln}-\text{O}-\text{Ln}$ angles are $119.2 \pm 0.1^\circ$, and the displacement of the oxide ion from the Ln_3 plane is $0.19 \pm 0.01 \text{ \AA}$.²³ This arrangement is best seen in the perspective views provided in Figures 3–5. On the other hand, the Li_3 -

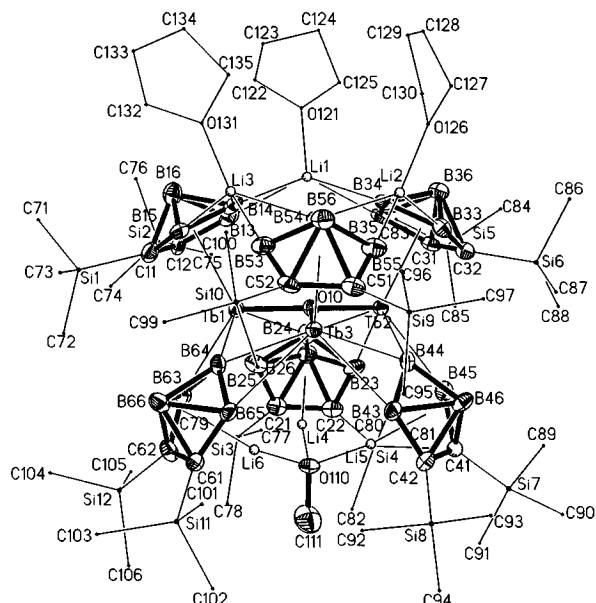


Figure 3. Perspective view of **3** showing the atom-numbering scheme with thermal ellipsoids drawn at the 25% probability level. The H atoms are omitted for clarity.

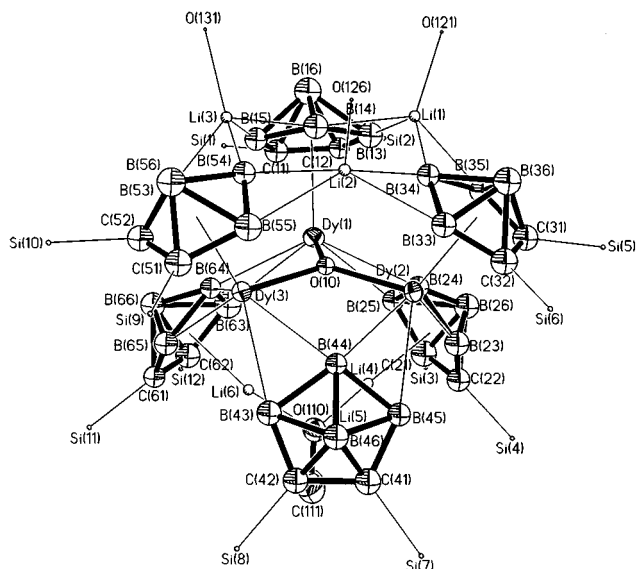


Figure 4. Perspective view of **4** showing the atom-numbering scheme with thermal ellipsoids drawn at the 25% probability level. The H atoms, the C atoms of the silyl groups, and the THF molecules are omitted for clarity.

OMe unit, located below the Ln_3 plane in Figure 1, can best be described as a distorted tetrahedral arrangement of the three lithiums and the Me unit about a central oxygen; the $\text{Li}-\text{O}-\text{Li}$ angles are $105.6 \pm 1.0^\circ$, while the $\text{Li}-\text{O}-\text{Me}$ angles average $113.1 \pm 0.9^\circ$ (see Figure 5). There is an additional Li_3 plane above the lanthanides that involves the three lithium atoms that are *exo*-polyhedrally bridged to adjacent boron atoms in the C_2B_3 faces of the two neighboring lanthanacarboranes. The structures of the clusters are such that the nine metal atoms form a tapered tricapped trigonal prism with the lanthanides occupying the capping positions. The M_3 planes are essentially parallel to one another; the average $[\text{Li}(1)-\text{Li}(2)-\text{Li}(3)]-[\text{Ln}(1)-\text{Ln}(2)-\text{Ln}(3)]$ dihedral angle is $1.0 \pm 0.1^\circ$, while the $[\text{Ln}(1)-\text{Ln}(2)-\text{Ln}(3)]-[\text{Li}(4)-\text{Li}(5)-\text{Li}(6)]$ angle is $1.5 \pm 0.5^\circ$. The average Li -carborane centroid (Cnt) distance in each lithiacarborane unit of **1–5** is $1.85 \pm 0.01 \text{ \AA}$,

(23) Whenever average values of a measured parameter are given, the uncertainties quoted are the average deviations.

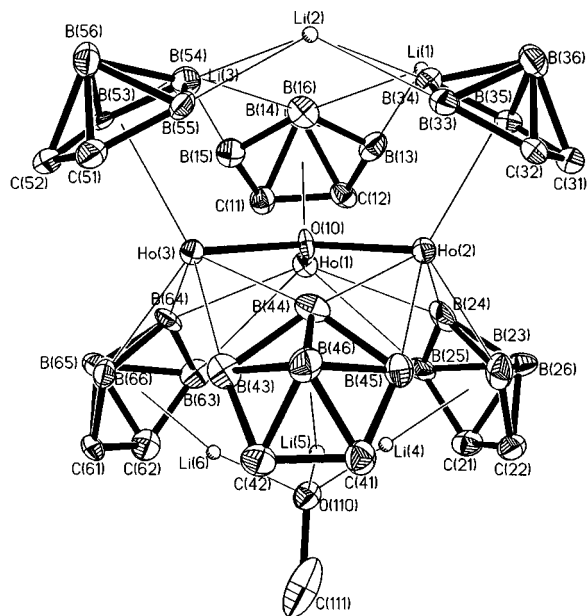


Figure 5. Perspective view of **5** showing the atom numbering scheme with thermal ellipsoids drawn at the 25% probability level. The H atoms, as well as the *exo*-polyhedral silyl groups and the THF molecules, are omitted for clarity.

which is shorter than the value of 1.906 Å found for the corresponding TMEDA-solvated dilithiacarborane, *closo-exo*-4,5-[(μ -H)₂Li(TMEDA)]-1-Li(TMEDA)-2,3-(SiMe₃)₂-2,3-C₂B₄H₄.^{13b} Evidently, the bulk of the large TMEDA group solvating the capping lithium in the latter compound promotes slightly longer Li–C_{nt} distances. The bridging Li(1–3)–B distances in compounds **1–5** range from 2.229 to 2.436 Å, which spans the average value of 2.235 ± 0.008 Å found for the bridging lithium–boron distances in the TMEDA-solvated dilithiacarborane.^{13b} Thus, even though the lithiacarborane units in compounds **1–5** are involved in extensive cluster formation, their internal geometries are not too different from that of the monomeric dilithiacarborane precursor.^{13b} The average Sm–O(10) distance in **1** is 2.211 ± 0.008 Å, which is slightly greater than the value of 2.094 Å found in the (η^5 -C₅Me₅)₂Sm–O–Sm(η^5 -C₅Me₅)₂ complex,¹⁹ while the Gd–O(10) distances of 2.193 ± 0.010 Å found in **2** are somewhat smaller than the 2.42 Å reported for the average Gd–(μ^5 -O) distance in {[(η^5 -C₅H₅)Gd]₅(μ_2 -OMe)₄(μ_3 -OMe)₄(μ_5 -O)}.²⁴ These observations are all consistent with the Ln–O interaction being predominantly ionic. The variation in the Ln–C_{nt} distances in compounds **1–5** can be successfully accounted for by considering the change in the ionic radii of the Ln(III) ions in going from Sm to Ho.²⁵ This type of rationale for bond length variations was one of the structural criteria suggested by Raymond and Eigenbrot for classifying ligand–metal interactions as predominantly ionic, rather than covalent.²⁶ Assuming that the metal–ligand bond distances in such complexes should be equal to the sums of the ionic radii of the metal and the ligand, these authors were able to calculate the effective ionic radii of several π -type donor ligands. For example, from the measured metal–carbon distances in a number of cyclopentadienyllanthanide and -actinide complexes they calculated the ionic radius of Cp[−] to be 1.64 ± 0.04

(24) Schumann, H.; Kociok-Köhn, G.; Loebel, J. *Z. Anorg. Allg. Chem.* **1990**, *581*, 69.

(25) Shannon, R. D. *Acta Crystallogr., Sect A* **1976**, *32*, 751.

Å.²⁶ Using the same approach, Hawthorne and co-workers obtained an ionic radius of 1.656 Å for [C₂B₉H₁₁]^{2−} in the {[C₂B₉H₁₁]₂Sm(THF)₂}[−] ion.⁶ From the Ln–C₂B₃ atom distances in **1–5**, and the ionic radii of the eight-coordinate Ln(III) ions given by Shannon,²⁵ the effective ionic radii of the carboranes in **1–5** were found to be 1.548, 1.554, 1.540, 1.547, and 1.548 Å, respectively.²⁷ The constancy of these calculated radii is further verification of the essentially ionic nature of the Ln–carborane bonds found in compounds **1–5**.

Structures of 6 and 7. The solid state structure of **6**, shown in Figure 6, is that of a dimanganese complex in which one metal atom, Mn(1), occupies the apical position in a *commo*-manganacarborane, while the other, Mn(2), is involved in an *exo*-polyhedral bridge between the two carborane cages. The structure of this compound is analogous to that of the diiron carborane [(CH₃)₂C₂B₄H₄]₂Fe₂[(OCH₃)₂C₂H₄] reported some time ago by Grimes and co-workers.²⁸ However, unlike the diiron complex, **6** is stable toward air. The bond distances given in Table 8 show that the two carborane ligands are η^5 -bonded to Mn(1), with average Mn–C₂B₃ atom distances of 2.181 ± 0.038 and 2.186 ± 0.064 Å, respectively, for the lower and upper cages shown in Figure 6. Within the limits of experimental errors, the C₂B₃ faces of the carboranes are planar and are parallel to one another. The second manganese, Mn(2), is η^2 -bonded to adjacent borons on the carborane bonding faces, with bond distances ranging from 2.327 Å, for Mn(2)–B(14), to 2.485 Å, for Mn(2)–B(23). It is of interest to compare the structure of **6** to that of the trimanganacarborane cluster {*commo*-Mn₃[2,3-(SiMe₃)₂-2,3-C₂B₄H₄]₄}^{3−} that was obtained from the direct reaction of MnCl₂ with the dilithiacarborane precursors of **1–5**. This product consisted of a central *commo*-manganacarborane complex that was bridged by two half-sandwich *closo*-manganacarboranes.²¹ The common nearest neighbor distances in this compound and **6** are quite similar. The Mn–C_{nt} and Mn–Mn distances in the trinuclear complex are 1.708 and 2.682 Å, respectively, which are quite close to the analogous distances of 1.714 ± 0.002 and 2.665 Å found in **6** (see Table 8). Despite these similarities, **6** is not just a fragment of the larger trinuclear complex. The relative orientation of the two carborane cages of the central *commo*-manganacarboranes are quite different. In the trinuclear complex the two carborane cages are eclipsed, resulting in a MnC₄B₈ moiety with C_{2v} symmetry. However, Figure 6 shows that the cages adopt a more staggered configuration so that the B(14)–C_{nt}(1)–C_{nt}(2)–B(24) dihedral angle is 62°, with the C(22) and B(15) atoms being almost over one another. With this configuration, it would not be possible for an additional Mn atom to bridge the two cages resulting in a trinuclear “butterfly” cluster.²¹

The structure of the cobaltacarborane, **7**, was found to be that of a linear sandwich complex. Figure 7 shows

(26) Raymond, K. N.; Eigenbrot, C. W., Jr. *Acc. Chem. Res.* **1980**, *13*, 276.

(27) Because of the bridging interactions of the lanthanides with the cages of the lithiacarborane units, the Ln coordination number in compounds **1–5** is not obvious. The coordination number of 8 was obtained by assuming that a bridge would effectively occupy two coordination sites, the carborane ligand three sites, and the oxide one site. If another coordination number is assumed, the absolute value of “ionic radius” of the carborane would change but not its constancy throughout the series **1–5**.

(28) Grimes, R. N.; Maynard, R. B.; Sinn, E.; Brewer, G. A.; Long, G. J. *J. Am. Chem. Soc.* **1982**, *104*, 5987.

Table 7. Selected Interatomic Distances (Å) and Angles (deg) for 1–5^a

Distances for 1							
Sm(1)··Sm(2)	3.806(2)	Sm(1)··Sm(3)	3.813(2)	Li(4)··Li(6)	2.986(23)	Li(5)··Li(6)	3.009(22)
Sm(2)··Sm(3)	3.827(2)	Sm(1)–Cnt(1)	2.405	Li(4)–Cnt(2)	1.84	Li(5)–Cnt(4)	1.85
Sm(2)–Cnt(3)	2.417	Sm(3)–Cnt(5)	2.417	Li(6)–Cnt(6)	1.86	Li(4)–O(110)	1.864(16)
Sm(1)–O(10)	2.203(5)	Sm(2)–O(10)	2.207(5)	Li(5)–O(110)	1.851(18)	Li(6)–O(110)	1.844(18)
Sm(3)–O(10)	2.224(5)	Li(4)··Li(5)	2.961(21)				
Distances for 2							
Gd(1)··Gd(2)	3.772(2)	Gd(1)··Gd(3)	3.778(2)	Li(4)··Li(6)	2.961(30)	Li(5)··Li(6)	2.937(26)
Gd(2)··Gd(3)	3.787(2)	Gd(1)–Cnt(1)	2.382	Li(4)–Cnt(2)	1.83	Li(5)–Cnt(4)	1.86
Gd(2)–Cnt(3)	2.398	Gd(3)–Cnt(5)	2.400	Li(6)–Cnt(6)	1.86	Li(4)–O(110)	1.879(22)
Gd(1)–O(10)	2.199(6)	Gd(2)–O(10)	2.199(6)	Li(5)–O(110)	1.809(22)	Li(6)–O(110)	1.839(21)
Gd(3)–O(10)	2.177(6)	Li(4)··Li(5)	2.962(27)				
Distances for 3							
Tb(1)··Tb(2)	3.7520(12)	Tb(1)··Tb(3)	3.7526(12)	Li(4)··Li(6)	2.969(14)	Li(5)··Li(6)	2.955(14)
Tb(2)··Tb(3)	3.7621(10)	Tb(1)–Cnt(1)	2.358	Li(4)–Cnt(2)	1.84	Li(5)–Cnt(4)	1.84
Tb(2)–Cnt(3)	2.374	Tb(3)–Cnt(5)	2.374	Li(6)–Cnt(6)	1.84	Li(4)–O(110)	1.842(11)
Tb(1)–O(10)	2.185(3)	Tb(2)–O(10)	2.170(3)	Li(5)–O(110)	1.849(11)	Li(6)–O(110)	1.861(11)
Tb(3)–O(10)	2.173(3)	Li(4)··Li(5)	2.941(14)				
Distances for 4							
Dy(1)··Dy(2)	3.726(2)	Dy(1)··Dy(3)	3.725(2)	Li(4)··Li(6)	2.830(52)	Li(5)··Li(6)	2.924(49)
Dy(2)··Dy(3)	3.742(2)	Dy(1)–Cnt(1)	2.326	Li(4)–Cnt(2)	1.90	Li(5)–Cnt(4)	1.84
Dy(2)–Cnt(3)	2.373	Dy(3)–Cnt(5)	2.368	Li(6)–Cnt(6)	1.90	O(110)–Li(4)	1.782(40)
Dy(1)–O(10)	2.184(10)	Dy(2)–O(10)	2.153(6)	O(110)–Li(5)	1.848(43)	O(110)–Li(6)	1.793(36)
Dy(3)–O(10)	2.186(10)	Li(4)··Li(5)	2.860(52)				
Distances for 5							
Ho(1)··Ho(2)	3.713(1)	Ho(1)··Ho(3)	3.712(1)	Li(4)··Li(6)	2.920(34)	Li(5)··Li(6)	2.939(30)
Ho(2)··Ho(3)	3.718(1)	Ho(1)–Cnt(1)	3.327	Li(4)–Cnt(2)	1.85	Li(5)–Cnt(5)	1.85
Ho(2)–Cnt(3)	2.350	Ho(3)–Cnt(5)	2.350	Li(6)–Cnt(6)	1.84	Li(4)–O(110)	1.830(25)
Ho(1)–O(10)	2.169(6)	Ho(2)–O(10)	2.153(6)	Li(5)–O(110)	1.833(25)	Li(6)–O(110)	1.863(22)
Ho(3)–O(10)	2.140(6)	Li(4)··Li(5)	2.872(31)				
Angles for 1							
Sm(2)··Sm(1)··Sm(3)	60.3(1)	Sm(1)··Sm(2)··Sm(3)	59.9(1)	Li(4)–O(110)–Li(5)	105.7(8)	Li(4)–O(110)–Li(6)	107.2(7)
Sm(1)··Sm(3)··Sm(2)	59.8(1)	Sm(1)–O(10)–Sm(2)	119.3(2)	Li(5)–O(110)–Li(6)	109.0(8)	Li(4)–O(110)–C(111)	114.0(9)
Sm(1)–O(10)–Sm(3)	118.9(2)	Sm(2)–O(10)–Sm(3)	119.4(2)	Li(5)–O(110)–C(111)	112.9(8)	Li(6)–O(110)–C(111)	107.8(9)
Angles for 2							
Gd(2)··Gd(1)··Gd(3)	60.2(1)	Gd(1)··Gd(2)··Gd(3)	60.0(1)	Li(4)··Li(6)··Li(5)	60.3(6)	Li(4)–O(110)–Li(5)	106.8(10)
Gd(1)··Gd(3)··Gd(2)	59.8(1)	Gd(1)–O(10)–Gd(2)	118.1(3)	Li(4)–O(110)–Li(6)	105.5(9)	Li(5)–O(110)–Li(6)	107.2(10)
Gd(1)–O(10)–Gd(3)	119.4(3)	Gd(2)–O(10)–Gd(3)	119.9(2)	Li(4)–O(110)–C(111)	112.5(12)	Li(5)–O(110)–C(111)	114.5(9)
Li(5)··Li(4)··Li(6)	59.5(6)	Li(4)··Li(5)··Li(6)	60.2(7)	Li(6)–O(110)–C(111)	109.8(11)		
Angles for 3							
Tb(2)··Tb(1)··Tb(3)	60.17(2)	Tb(1)··Tb(2)··Tb(3)	59.92(2)	Li(5)··Li(6)··Li(4)	59.5(3)	Li(4)–O(110)–C(111)	116.1(5)
Tb(1)··Tb(3)··Tb(2)	59.91(2)	Tb(2)–O(10)–Tb(3)	120.1(2)	Li(5)–O(110)–C(111)	113.7(5)	Li(6)–O(110)–C(111)	108.5(5)
Tb(2)–O(10)–Tb(1)	119.0(2)	Tb(3)–O(10)–Tb(1)	118.9(2)	Li(4)–O(110)–Li(5)	105.6(5)	Li(4)–O(110)–Li(6)	106.6(5)
Li(5)··Li(4)··Li(6)	60.0(3)	Li(4)··Li(5)··Li(6)	60.5(3)	Li(5)–O(110)–Li(6)	105.6(5)		
Angles for 4							
Dy(2)··Dy(1)··Dy(3)	60.3(1)	Dy(1)··Dy(2)··Dy(3)	59.8(1)	Li(4)··Li(6)··Li(5)	59.6(12)	Li(4)–O(110)–Li(5)	104.0(20)
Dy(1)··Dy(3)··Dy(2)	59.9(1)	Dy(1)–O(10)–Dy(2)	120.1(5)	Li(4)–O(110)–Li(6)	104.7(17)	Li(5)–O(110)–Li(6)	106.8(19)
Dy(1)–O(10)–Dy(3)	117.0(5)	Dy(2)–O(10)–Dy(3)	120.9(4)	Li(4)–O(110)–C(111)	112.8(21)	Li(5)–O(110)–C(111)	117.2(18)
Li(5)··Li(4)··Li(6)	61.8(13)	Li(4)··Li(5)··Li(6)	58.6(12)	Li(6)–O(110)–C(111)	110.4(19)		
Angles for 5							
Ho(2)··Ho(1)··Ho(3)	60.1(1)	Ho(1)··Ho(2)··Ho(3)	59.9(1)	Li(4)··Li(6)··Li(5)	58.7(7)	Li(4)–O(110)–Li(5)	103.3(12)
Ho(1)··Ho(3)··Ho(2)	60.0(1)	Ho(1)–O(10)–Ho(2)	118.5(3)	Li(4)–O(110)–Li(6)	104.5(11)	Li(5)–O(110)–Li(6)	105.3(12)
Ho(1)–O(10)–Ho(3)	119.0(3)	Ho(2)–O(10)–Ho(3)	120.0(3)	Li(4)–O(110)–C(111)	118.0(12)	Li(5)–O(110)–C(111)	115.8(10)
Li(5)··Li(4)··Li(6)	61.0(8)	Li(4)··Li(5)··Li(6)	60.3(8)	Li(6)–O(110)–C(111)	108.6(12)		

^a Cnt(1) = the centroid of the C2B3 basal ring of C(11), C(12), ..., and B(16); Cnt(2) = the centroid of C(21), C(22), ..., and B(26); ...Cnt(6) = the centroid of C(61), C(62), ..., and B(66).

that a Co(III) metal occupies the apical positions of two η^5 -bonded carborane ligands, with the cage carbons directly opposite to one another, giving a CoC₄B₈ unit of *C_{2h}* symmetry. This orientation of the carborane ligands has been found in a number of main group and transition metal *commo*-metallacarboranes.^{1,29–31} The

respective Co–C(2) and average Co–B(4,5) bond distances of 2.026 and 2.07 ± 0.02 Å (see Table 8) are similar to the equivalent distances of 2.057 ± 0.008 and 2.107 ± 0.004 Å found for the [1,1'-*commo*-Co{2,3-(Et)₂-2,3-C₂B₄H₄}₂][−] in {[Cp₂Co][Co(Et₂C₂B₄H₄)₂]}.³² While the Co–C₂B₃ bond distances are similar, compound **7** differs from [Co(Et₂C₂B₄H₄)₂][−] in that the two carborane cages in the latter compound are nearly eclipsed and

(29) (a) Siriwardane, U.; Islam, M. S.; West, T. A.; Hosmane, N. S.; Maguire, J. A.; Cowley, A. H. *J. Am. Chem. Soc.* **1987**, *109*, 4800. (b) Islam, M. S.; Siriwardane, U.; Hosmane, N. S.; Maguire, J. A.; de Meester, P.; Chu, S. S. C. *Organometallics* **1987**, *6*, 1936.

(30) (a) Rees W. S., Jr.; Schubert, D. M.; Knobler, C. B.; Hawthorne, M. F. *J. Am. Chem. Soc.* **1986**, *108*, 5369. (b) Schubert, D. M.; Rees, W. S., Jr.; Knobler, C. B.; Hawthorne, M. F. *Organometallics* **1990**, *9*, 2938.

(31) Oki, A. R.; Zhang, H.; Maguire, J. A.; Hosmane, N. S.; Ro, H.; Hatfield, W. E. *Organometallics* **1991**, *10*, 2996. Oki, A. R.; Zhang, H.; Maguire, J. A.; Hosmane, N. S.; Ro, H.; Hatfield, W. E.; Moscherosch, M.; Kaim, W. *Organometallics* **1992**, *11*, 4202.

(32) Meng, X.; Waterworth, S.; Sabat, M.; Grimes, R. N. *Inorg. Chem.* **1993**, *32*, 3188.

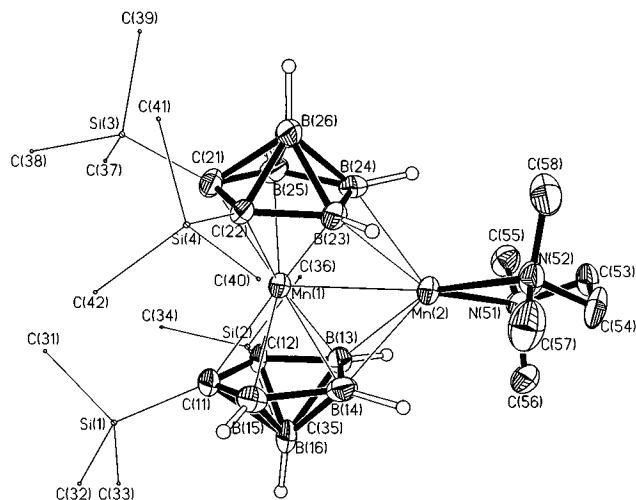


Figure 6. Perspective view of 4,4',5,5'-Mn(TMEDA)-1,1'-*commo*-Mn[2,3-(SiMe₃)₂-2,3-C₂B₄H₄]₂ (**6**) showing the atom-numbering scheme with thermal ellipsoids drawn at the 40% probability level. The methyl and methylene H's are not shown for clarity. The atoms of the silyl groups are drawn with circles of arbitrary radii.

Table 8. Selected Interatomic Distances (Å) and Angles (deg) for 6 and 7^a

Distances for 6			
Mn(1)–Mn(2)	2.665(2)	Mn(1)–Cnt(1)	1.712
Mn(1)–Cnt(2)	1.717	Mn(1)–C(11)	2.227(6)
Mn(1)–C(12)	2.131(7)	Mn(1)–B(13)	2.137(8)
Mn(1)–B(14)	2.193(8)	Mn(1)–B(15)	2.219(8)
Mn(1)–C(21)	2.220(6)	Mn(1)–C(22)	2.090(6)
Mn(1)–B(23)	2.123(8)	Mn(1)–B(24)	2.225(7)
Mn(1)–B(25)	2.274(8)	Mn(2)–B(13)	2.458(8)
Mn(2)–B(14)	2.340(8)	Mn(2)–B(23)	2.485(7)
Mn(2)–B(24)	2.327(7)	Mn(2)–N(51)	2.246(5)
Mn(2)–N(52)	2.261(5)		
Distances for 7			
Co–Cnt(3)	1.608	Co–C(2)	2.026(8)
Co–B(4)	2.09(2)	Co–B(5)	2.15(2)
Li–N(21)	2.064(11)	C(2)–C(2) ¹	1.53(2)
C(2)–B(4)	1.61(2)	C(2)–B(7)	1.80(2)
B(4)–B(5)	1.50(2)	B(4)–B(7)	1.78(2)
B(5)–B(7)	1.53(2)	C(31)–C(31) ²	1.22(5)
C(31)–C(32)	1.32(3)		
Angles for 6			
Cnt(1)–Mn(1)–Cnt(2)	175.7	Mn(2)–Mn(1)–Cnt(1)	88.8
Mn(2)–Mn(1)–Cnt(2)	88.7	Mn(1)–Mn(2)–N(51)	138.1(2)
Mn(1)–Mn(2)–N(52)	141.3(1)	N(51)–Mn(2)–N(52)	80.5(2)
Angles for 7			
Cnt(3)–Co–Cnt(3a)	180.00	N(21)–Li–N(21) ³	98.2(7)
N(21)–Li–N(21) ⁴	115.4(4)		

^a Symmetry transformations used to generate equivalent atoms; (1) $x, y, -z$; (2) $-x+1, -y, z$; (3) $-x+1, -y+1, z$; (4) $y, -x+1, -z+1/2$.

are tilted so that their respective C₂B₃ faces form a dihedral angle of 5.3°.³² It was speculated that the eclipsed configuration and tilting leaves the BH vertices free to allow closer contact of the cobaltocenium ions which results in greater ion-pair electrostatic stabilization. Since the closest approach of the lithium cation to a cobaltacarborane atom is >8.0 Å, such a geometric distortion would not be expected in the structure of **7**.

Spectra. All compounds were characterized by infrared spectroscopy, the results of which are summarized in Table 2. With the exception of compound **7**, all show multiple peaks in the B–H stretching region. Such splittings have been observed in the IR spectra of the dilithium precursor, and other group 1 metallocarboranes, and were explained in terms of a M–H–B

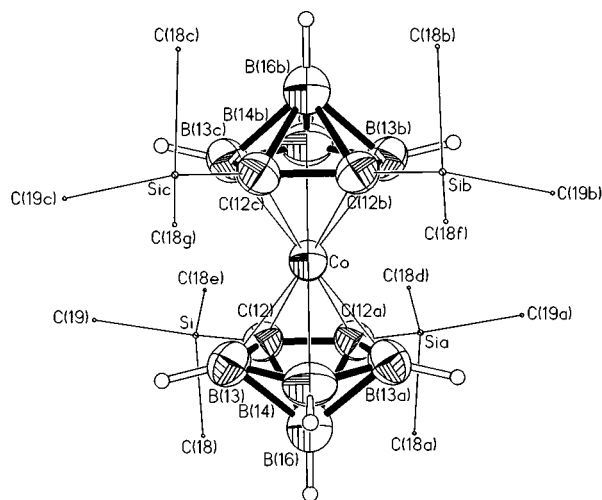


Figure 7. Perspective view of the anionic unit, {1,1'-*commo*-Co[2,3-(SiMe₃)₂-2,3-C₂B₄H₄]₂}⁻, of **7** showing the atom-numbering scheme with thermal ellipsoids drawn at the 40% probability level. The atoms of the silyl groups are drawn with circles of arbitrary radii, and the Li⁺(TMEDA)₂ cation is not shown for clarity.

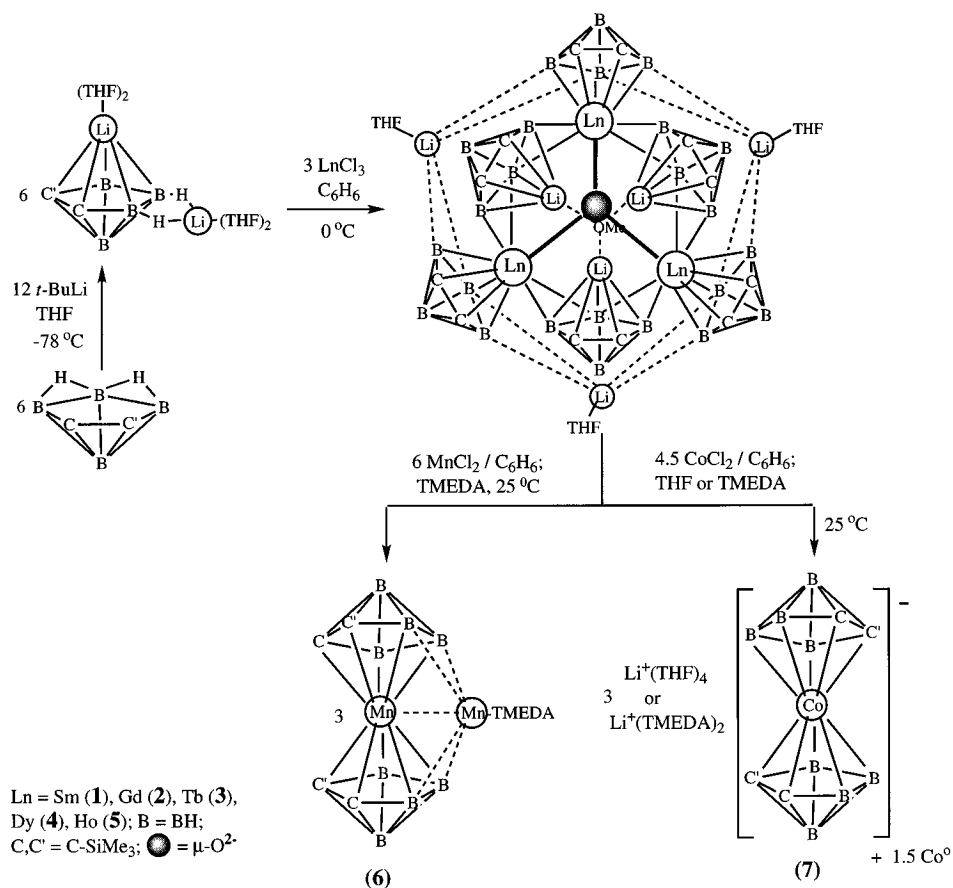
bridging interaction between an *exo*-polyhedral group 1 metal and two adjacent borons on the C₂B₃ carborane face.^{13b} Such bridging interactions, involving either a lithium or a lanthanide metal atom, are apparent in the crystal structures of compounds **1–5** (see Figures 1–5). The structure of the manganese complex, **6**, shown in Figure 6, also reveals a strong metal interaction with only one side of the C₂B₃ face. On the other hand, the cobaltacarborane, **7**, which does not have such metal–carborane interactions, shows only a single band in the B–H stretching region (see Table 2 and Figure 7).

Compounds **1**, **7**, and **7a** were also characterized by ¹H, ¹¹B, and ¹³C NMR spectroscopy. All spectra are consistent with the formulas given in the Experimental Section. The solution ¹¹B NMR spectrum of **7** is consistent with its solid-state structure, shown in Figure 7. The structure shows a CoC₄B₈ cage having C_{2h} symmetry, with the two cages being η⁵-bonded to the central cobalt atom. This results in three sets of boron atoms, two unique borons [B(14,14b)], four basal borons [B(13,13a,13b,13c)], and two apical borons [B(16,16b)], which is consistent with the experimental ¹¹B NMR spectrum of three peaks with 1:2:1 peak area ratios. The ¹¹B NMR pattern of **7** is also typical of that found for the pentagonal bipyramidal metallocarboranes, in that it shows an upfield resonance at δ = -8.90 ppm, due to the apical borons, with the downfield resonances at δ = 8.54 and 0.09 ppm being attributed to the borons in the C₂B₃ face.^{31,33,34} Since the ¹¹B NMR spectra of **7** and **7a** are essentially the same, it is safe to assume that Figure 7 also gives the correct structure of **7a**. Due to the paramagnetism of compounds **2–6**, meaningful NMR spectra of these compounds could not be obtained. Because of more rapid relaxation, broad, but resolvable, NMR spectra were obtained for the samaracarborane, **1**. However, unlike those of compound **7**, these spectra are not easily rationalized on the basis of its solid-state structure, shown in Figure 1. While the ¹H and ¹³C

(33) Zhang, H.; Wang, Y.; Saxena, A. K.; Oki, A. R.; Maguire, J. A.; Hosmane, N. S. *Organometallics* **1993**, *12*, 3933.

(34) Maguire, J. A.; Fagner, J. S.; Siriwardane, U.; Baniewicz, J. J.; Hosmane, N. S. *Struct. Chem.* **1990**, *1*, 583 and references therein.

Scheme 1



spectra show peaks due to the various groups in the formula, the number of such resonances do not necessarily correspond to those expected from its structure. For example, while both the ^1H and ^{13}C NMR spectra indicate the presence of four different SiMe_3 groups, only two sets are apparent from its solid-state structure. The ^{11}B NMR spectra, which for other metallacarboranes have proved especially useful in structural determinations, present special difficulties. Figure 1 shows that the cluster contains six carborane cages, three η^5 -bonded to samarium atoms, while the other three are η^5 -bonded to lithiums; these should give rise to at least seven nonequivalent borons. However, the ^{11}B NMR spectrum of **1** shows only four resonances with peak area ratios of 1:1:1:1. The only attempt at assignments is to ascribe the peak at $\delta = -17.58$ ppm to the resonance of an apical boron, the main justification for this being that the apical boron resonances in most metallacarboranes are found in the 0 to -55 ppm region.^{31,33,34} Therefore, the spectra are presented for the purposes of qualitative identification only.

Acknowledgment. This work was supported in part by grants from the Texas Advanced Technology Program (003613006), the National Science Foundation (CHE-9400672), the Robert A. Welch Foundation (N-1016), and the donors of the Petroleum Research Fund, administered by the American Chemical Society.

Supporting Information Available: Tables of selected bond lengths and bond angles (Tables S-1 and S-2 for **1**, Tables S-5 and S-6 for **2**, Tables S-9 and S-10 for **3**, Tables S-13 and S-14 for **4**, Tables S-17 and S-18 for **5**, Table S-21 for **6**, and S-24 for **7**), anisotropic displacement parameters (Tables S-3, S-7, S-11, S-15, S-19, S-22, and S-25 for **1–7**, respectively), and H atom coordinates and isotropic displacement coefficients (Tables S-4, S-8, S-12, S-20, S-23, and S-26 for **1–3** and **5–7**, respectively) (69 pages). Ordering information is given on any current masthead page.

OM950691L